nature immunology

The transcription factor STAT5 is critical in dendritic cells for the development of T_H2 but not T_H1 responses

Bryan D Bell[1,2,6], Masayuki Kitajima[1,2,6], Ryan P Larson[1,2], Thomas A Stoklasek[1,2], Kristen Dang[1], Kazuhito Sakamoto[3], Kay-Uwe Wagner[3], Boris Reizis[4], Lothar Hennighausen[5] & Steven F Ziegler[1,2]

Dendritic cells (DCs) are critical in immune responses, linking innate and adaptive immunity. We found here that DC-specific deletion of the transcription factor STAT5 was not critical for development but was required for T helper type 2 (T_H2), but not T_H1, allergic responses in both the skin and lungs. Loss of STAT5 in DCs led to the inability to respond to thymic stromal lymphopoietin (TSLP). STAT5 was required for TSLP-dependent DC activation, including upregulation of the expression of costimulatory molecules and chemokine production. Furthermore, T_H2 responses in mice with DC-specific loss of STAT5 resembled those seen in mice deficient in the receptor for TSLP. Our results show that the TSLP-STAT5 axis in DCs is a critical component for the promotion of type 2 immunity at barrier surfaces.

© 2013 Nature America, Inc. All rights reserved.

Three cytokine pathways have been identified as being important for the development of dendritic cells (DCs) both *in vivo* and *in vitro*. Of those, only the pathway involving the cytokine Flt3L seems to be nonredundant, as deletion of Flt3L results in 90% fewer DCs[1,2]. The lack of DC development in Flt3L-deficient mice seems to be due to lack of activation of the transcription factor STAT3 (ref. 3). Further evidence of the importance of STAT3 in DC development has been provided by studies showing that ectopic expression of STAT3 in non-DC hematopoietic progenitors results in development of both conventional DCs (cDCs) and plasmacytoid DCs (pDCs)[4]. However, the influence of STAT3 may be restricted to Flt3 signaling, as *in vitro* DC differentiation driven by the cytokine GM-CSF is unaffected by STAT3 deficiency[3].

A similar nonredundant role for the transcription factor STAT5 in DC development is less clear. GM-CSF can activate both STAT5 and STAT3, and GM-CSF-activated STAT5 inhibits the transcription of *Irf8* (ref. 5), which encodes a transcription factor (IRF8) shown to be critical for the development of pDCs and CD8α$^+$ cDCs *in vivo*[6]. In addition, GM-CSF-activated STAT5 also inhibits the Ets family transcription factor Spi-B, the transcription factor IRF7, the receptor tyrosine kinase Flt3 and Toll-like receptor 9, all factors involved in pDC development[1,7]. Thus, one potential role for STAT5 is to promote cDC differentiation through inhibition of pDC development.

After maturation of DCs, STAT5 is activated by many cytokines, including GM-CSF and thymic stromal lymphopoietin (TSLP). TSLP is expressed by a variety of cell types and signals via a heterodimer of the interleukin 7 (IL-7) receptor α-chain (IL-7Rα (CD127)) and the unique TSLP receptor chain (TSLPR) [8,9]. IL-7Rα and TSLPR use the signaling kinases Jak1 and Jak2, respectively, for the activation of STAT proteins in human DCs and mouse CD4$^+$ T lymphocytes[10,11]. In human DCs, TSLP has been shown to activate STAT1, STAT3, STAT4, STAT5 and STAT6 (ref. 11). Studies of mice have shown that stimulation with TSLP leads to the activation of STAT5 and the induction of STAT5-responsive genes[12–16].

Several cell types have been shown to be TSLP responsive, including DCs, Langerhans cells (LCs), T cells, B cells, basophils, eosinophils and monocytes-macrophages[8]. *In vivo* studies have shown that both DCs and CD4$^+$ T cells are important for TSLP-dependent responses[17–19]. Furthermore, high concentrations of TSLP are associated with allergic diseases in humans and are important for type 2 inflammatory responses in mice[8,20].

Here we assessed the consequence of Cre recombinase–mediated deletion of STAT5 on DC homeostasis and various TSLP-dependent and TSLP-independent T helper type 2 (T_H2) and T_H1 responses *in vivo*, respectively. We found that STAT5 was dispensable for normal homeostasis and function of DCs but was absolutely required for various models of TSLP-dependent T_H2 response–mediated atopic disorders. Notably, T_H1 responses were normal in mice that lacked STAT5 in DCs. The T_H2 defects were due to many factors, including less migration and activation of antigen-bearing DCs after sensitization and a concomitantly diminished ability to drive the proliferation of antigen-specific T cells and production of T_H2 cytokines. Together our results emphasize the importance of STAT5 in DCs during TSLP-mediated T_H2 responses and suggest that DCs are a critical *in vivo* target of TSLP.

[1]Immunology Program, Benaroya Research Institute at Virginia Mason, Seattle, Washington, USA. [2]Department of Immunology, University of Washington School of Medicine, Seattle, Washington, USA. [3]Eppley Institute for Research in Cancer and Allied Diseases, University of Nebraska Medical Center, Omaha, Nebraska, USA. [4]Department of Microbiology and Immunology, Columbia University Medical Center, New York, New York, USA. [5]Laboratory of Genetics and Physiology, US National Institutes of Health, Bethesda, Maryland, USA. [6]These authors contributed equally to this work. Correspondence should be addressed to S.F.Z. (sziegler@benaroyaresearch.org).

Received 13 September 2012; accepted 8 January 2013; published online 24 February 2013; doi:10.1038/ni.2541

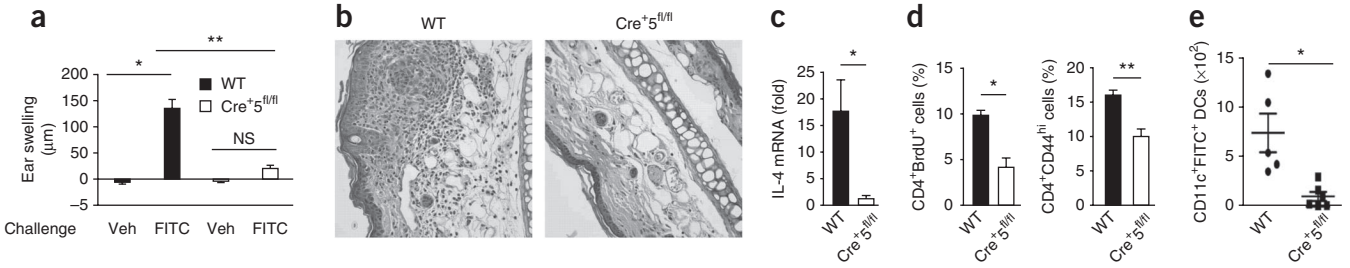

Figure 1 Diminished T_H2 CHS Cre$^+$*Stat5*$^{fl/fl}$ mice. (**a**) Change in ear thickness in wild-type (BALB/c control) mice (WT) and Cre$^+$*Stat5*$^{fl/fl}$ mice (Cre$^+$5$^{fl/fl}$) sensitized with 0.5% FITC (on the abdomen) on day 0, followed by measurement of baseline ear thickness on day 6, then challenge with vehicle (Veh) or FITC (horizontal axis) and analysis 24 h after challenge. $*P = 0.0001$ and $**P = 0.0003$ (two-way analysis of variance (ANOVA)). (**b**) Hematoxylin- and eosin-stained ear sections ($n = 5$ per genotype) from wild-type and Cre$^+$*Stat5*$^{fl/fl}$ mice sensitized and challenged with FITC, fixed 24 h after challenge. Original magnification, ×400. (**c**) IL-4 mRNA in ear tissue excised and processed 24 h after challenge as in **a**; results are normalized to those of HPRT (control mRNA) and are presented relative to those of vehicle-challenged wild-type mice. $*P = 0.024$ (Student's *t*-test). (**d**) Frequency of BrdU$^+$ or CD4$^+$CD44^{hi} T cells in skin-draining lymph nodes 24 h after challenge as in **b**. $*P = 0.005$ and $**P = 0.012$ (Student's *t*-test). (**e**) CD11c$^+$FITC$^+$ DCs (top) and mean fluorescence intensity (MFI) of CD86 on CD11c$^+$FITC$^+$ DCs (bottom) in axillary and inguinal lymph nodes 24 h after sensitization with 0.5% FITC (on the abdomen). Each symbol represents an individual mouse; small horizontal lines indicate the mean (and s.e.m.). $*P = 0.049$ and $**P = 0.005$ (Student's *t*-test). Data are representative of five independent experiments with four to six mice per group (error bars, s.e.m.).

© 2013 Nature America, Inc. All rights reserved.

RESULTS

Normal DC homeostasis does not require STAT5

To assess the requirement for STAT5 in DCs to promote T_H1 and T_H2 immune responses, we first generated mice with *lox*P-flanked *Stat5* alleles that also expressed Cre recombinase from the DC-specific gene *Cd11c* (CD11c-Cre$^+$*Stat5*$^{fl/fl}$ (Cre$^+$*Stat5*$^{fl/fl}$) mice) or did not express Cre from *Cd11c* (CD11c-Cre$^-$*Stat5*$^{fl/fl}$ (Cre$^-$*Stat5*$^{fl/fl}$) mice)[5,20,21]. We then assessed the consequences of Cre-mediated deletion of *Stat5*$^{fl/fl}$ in spleens. Total cellularity was similar in Cre$^-$*Stat5*$^{fl/fl}$ and Cre$^+$*Stat5*$^{fl/fl}$ mice, as was with the frequency of natural killer cells, macrophages, neutrophils and lymphocytes (**Supplementary Fig. 1a**). The spleen has three main populations of DCs: pDCs (CD11c$^+$CD11b$^-$PDCA1$^+$), CD8$^+$ DCs (CD11c$^+$CD11b$^-$PDCA1$^-$CD8α$^+$CD4$^-$) and CD4$^+$ DCs (CD11c$^+$CD11b$^+$PDCA1$^-$CD8$^-$CD4$^+$). The frequency and absolute number of each DC population was similar in Cre$^-$*Stat5*$^{fl/fl}$ and Cre$^+$*Stat5*$^{fl/fl}$ spleens (**Supplementary Fig. 1b**). Lineage-tracing studies showed that the activity of CD11c-Cre in the Cre$^+$ DCs (**Supplementary Fig. 1b**) correlated with the extent of germline recombination at the *Stat5* locus (**Supplementary Fig. 1c**). CD8$^+$ DCs had the highest efficiency of *Stat5* deletion, whereas pDCs showed 50% deletion of *Stat5* in the germline (**Supplementary Fig. 1c**).

We analyzed DC subsets present in the epidermal and dermal layers of skin and skin-draining lymph nodes of Cre$^+$*Stat5*$^{fl/fl}$ mice. LCs constitute a homogenous subset of DCs that reside in the epidermis, and we detected only CD11b$^+$ LCs with high expression of major histocompatibility complex (MHC) class II (MHCII^{hi}) and expression of langerin (CD207$^+$) in Cre$^-$*Stat5*$^{fl/fl}$ and Cre$^+$*Stat5*$^{fl/fl}$ epidermis (**Supplementary Fig. 2a**,**b**). Four distinct steady-state dermal DC subsets have been identified[21]. First, CD207^{hi}CD11b^{int} (R1) cells correspond to migratory LCs en route to the skin-draining lymph nodes. Second, CD207$^+$CD11b$^-$DC (R2) cells correspond to the CD207$^+$ dermal DC subset. We found two CD207$^-$ dermal DC subsets, CD11b$^-$ and CD11b$^+$ (R3 and R4, respectively), in Cre$^-$*Stat5*$^{fl/fl}$ and Cre$^+$*Stat5*$^{fl/fl}$ dermis (**Supplementary Fig. 2a**). DCs in skin-draining lymph nodes are more heterogeneous, as they include blood-derived, lymphoid tissue–resident CD4$^+$ DCs, CD8$^+$ DCs, migratory LCs and dermal DCs[22]. In skin-draining lymph nodes, expression of MHC class II, CD207 and CD11b did not allow the discrimination of migratory LCs and dermal DCs, as both appeared as CD207$^+$CD11b$^{neg–lo}$ cells (R1-R2; **Supplementary Fig. 2c**). Skin-draining lymph nodes from Cre$^+$*Stat5*$^{fl/fl}$ mice were consistently smaller than those from Cre$^-$*Stat5*$^{fl/fl}$ mice (**Supplementary Fig. 2d**). However, there was an equally lower abundance of all lymph node cell populations, as the frequency of Cre$^+$*Stat5*$^{fl/fl}$ lymph node cell populations was similar to that of their *Stat5*$^{+/+}$ counterparts (**Supplementary Fig. 2e** and data not shown). Finally, over 90% of CD11c$^+$ DCs from the skin-draining lymph nodes were Cre$^+$ (**Supplementary Fig. 2f**), which suggested efficient CD11c-Cre activity in Cre$^+$*Stat5*$^{fl/fl}$ lymph nodes. In addition, TSLPR expression on epidermal DCs, dermal DCs and skin-draining lymph node DCs was the same in Cre$^-$*Stat5*$^{fl/fl}$ and Cre$^+$*Stat5*$^{fl/fl}$ mice (**Supplementary Fig. 2g**). Together these data showed that the loss of STAT5 in CD11c$^+$ cells did not preclude the development of any DC subset in the spleen, skin, lungs or lymph nodes and affected only the total cellularity of lymph nodes. Furthermore, loss of STAT5 did not lead to the overt autoimmune pathology of mice with specific deletion of STAT3 in DCs[23] (data not shown).

T_H2 contact hypersensitivity requires STAT5 in dermal DCs

Contact hypersensitivity (CHS) is an animal model for human allergic contact dermatitis[24]. It is divided into two distinct phases, sensitization and elicitation; the latter occurs after exposure of a previously unexposed site to antigen. The hapten FITC (fluorescein isothiocyanate) in combination with the phthalate ester DBP (dibutyl phthalate) induces a T_H2 response in mice[25,26]. To understand the role of STAT5 in DCs during a T_H2 response, we sensitized and challenged wild-type and Cre$^+$*Stat5*$^{fl/fl}$ mice with FITC-DBP. Ear swelling at 24 h after challenge was much less in Cre$^+$*Stat5*$^{fl/fl}$ mice than in wild-type mice (**Fig. 1a**). Correspondingly, challenged wild-type mice had a substantial cellular infiltrate, epidermal thickening and lesions, which were much less in challenged Cre$^+$*Stat5*$^{fl/fl}$ mice (**Fig. 1b**). Cre$^+$*Stat5*$^{fl/fl}$ mice had less IL-4 mRNA than did wild-type mice in the inflamed ears (**Fig. 1c**). In addition, the frequency of CD4$^+$ T cells positive for the thymidine analog BrdU or with high expression of the activation and memory marker CD44 in the skin-draining lymph nodes was lower in Cre$^+$*Stat5*$^{fl/fl}$ mice than in wild-type mice (**Fig. 1d**), which suggested an inability of STAT5-deficient DCs to activate antigen-specific T cells. We further observed significantly fewer FITC$^+$ DCs in the skin-draining lymph nodes and

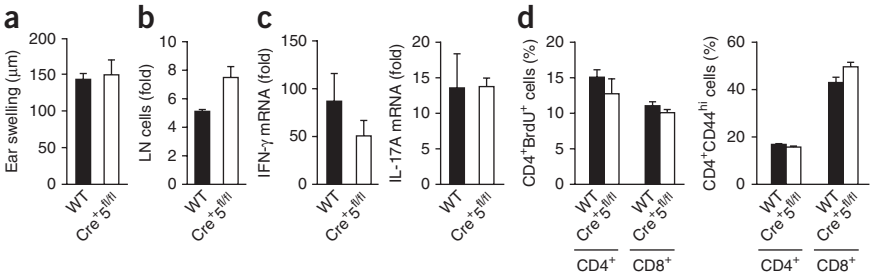

Figure 2 Normal T_H1-type CHS in Cre$^+$*Stat5*$^{fl/fl}$ mice. (**a**) Change in ear thickness in wild-type and Cre$^+$*Stat5*$^{fl/fl}$ mice sensitized on day 0 with DNFB (on the abdomen), followed by measurement of baseline ear thickness on day 6, then challenge with DNFB on the ear and analysis 24 h after challenge. (**b**) Cellularity of axillary and inguinal lymph nodes (LN; pooled) from wild-type (BALB/c) and Cre$^+$*Stat5*$^{fl/fl}$ mice challenged as in **a**, relative to that of nonsensitized, unchallenged mice of the matching genotype. (**c**) IFN-γ and IL-17A mRNA in ear tissue excised and processed 24 h after challenge as in **a** (presented as in **Fig. 1c**). (**d**) Frequency of BrdU$^+$ or CD4$^+$CD44^{hi} T cells in skin-draining lymph nodes 24 h after challenge as in **a**. Data are representative of three independent experiments with four to five mice per group (error bars, s.e.m.).

significantly lower expression of the costimulatory molecule CD86 (B7-2) on FITC$^+$ DCs from Cre$^+$*Stat5*$^{fl/fl}$ mice than in their wild-type counterparts (**Fig. 1e**), which suggested a possible mechanism for the diminished proliferation of CD4$^+$ T cells.

To determine whether the lack of response in the FITC-DBP model was due to a general DC defect, we used a second CHS model in which a T_H1 response is induced by sensitization and challenge with the hapten DNFB (2,4-dinitrofluorobenzene)[24]. In both wild-type and Cre$^+$*Stat5*$^{fl/fl}$ mice, DNFB-induced CHS lead to substantial ear-swelling (**Fig. 2a**). Furthermore, whereas the cellularity of skin-draining lymph nodes of Cre$^+$*Stat5*$^{fl/fl}$ mice at steady state was consistently less than that of wild-type mice, the enhanced cellularity after DNFB treatment was not significantly different for wild-type and Cre$^+$*Stat5*$^{fl/fl}$ mice (**Fig. 2b**). There was also no difference in the expression of interferon-γ (IFN-γ) mRNA and IL-17 mRNA, the proliferation of CD4$^+$ T cells and CD8$^+$ T cells and expression of CD44 in challenged wild-type and Cre$^+$*Stat5*$^{fl/fl}$ mice (**Fig. 2c**,**d**).

During sensitization, both LC and dermal DCs take up hapten-protein complexes and migrate to skin-draining lymph nodes. To determine if loss of the T_H2 CHS response was due to the absence of STAT5 in LCs or dermal DCs, we crossed mice expressing Cre from the promoter of the human encoding langerin (Lang-Cre mice), which restricts Cre expression to mouse LCs[27], with *Stat5*$^{fl/fl}$ mice to generate Lang-Cre$^-$*Stat5*$^{fl/fl}$ and Lang-Cre$^+$*Stat5*$^{fl/fl}$ mice. Loss of STAT5 in LCs did not affect the number or distribution of LCs in the epidermis or migratory LCs in the dermis (**Fig. 3a**,**b**). After sensitization and challenge with FITC-DBP, Lang-Cre$^+$*Stat5*$^{fl/fl}$ mice had ear swelling, as well as other aspects of the response, similar to that of wild-type and Lang-Cre$^-$*Stat5*$^{fl/fl}$ control mice (**Fig. 3c**,**d**). Together these results demonstrated a requirement for STAT5 in dermal DC subsets for the control of T_H2 skin responses.

T_H2 cell–dependent lung responses require STAT5 in DCs

To determine if STAT5 in DCs is generally required for T_H2 inflammation, we studied two models of airway inflammation. First we assessed the requirement for STAT5 in DCs during ovalbumin (OVA)-induced airway inflammation[28]. On day 10, as expected, bronchoalveolar lavage (BAL) fluid from wild-type mice had a significantly greater cellularity than that of Cre$^+$*Stat5*$^{fl/fl}$ mice, and it was mainly eosinophilic and characterized by the production of T_H2 cytokines (**Fig. 4a**,**b**). However, Cre$^+$*Stat5*$^{fl/fl}$ mice recruited fewer eosinophils to the bronchoalveolar space and produced less IL-4 and more IFN-γ in the mediastinal lymph than did wild-type mice (**Fig. 4a**,**b**).

To determine whether the absence of STAT5 in CD11c$^+$ DCs led to an inability of the mice to respond to general lung inflammation, we infected mice with influenza A virus. Infection with influenza A virus is dominated by proinflammatory and T_H1 response–associated cytokines. We infected wild-type and Cre$^+$*Stat5*$^{fl/fl}$ mice with influenza A virus (strain A/Aichi/68 (H3N2) and, as expected, found that wild-type mice lost weight but began to recover after 5 d,

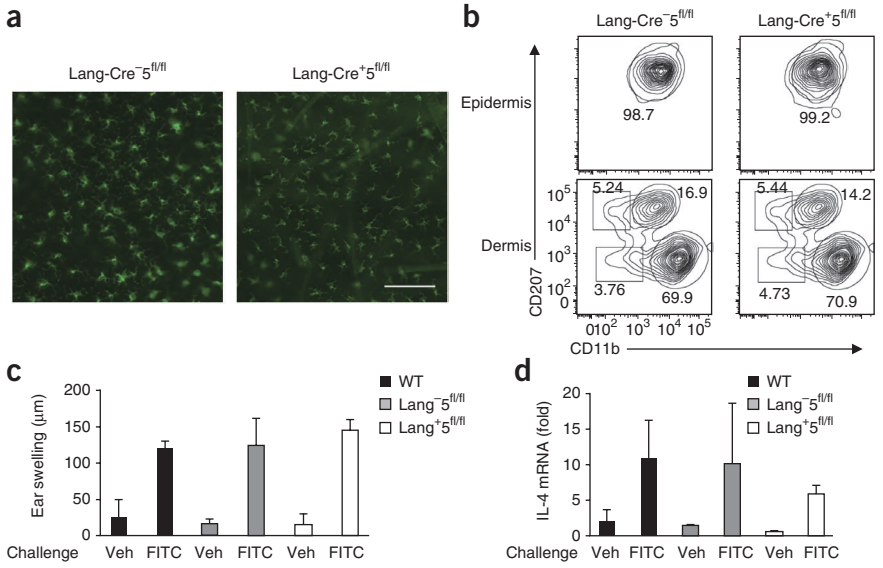

Figure 3 STAT5 is not required in LCs for T_H2-type CHS. (**a**) Fluorescence microscopy of MHC class II in epidermal sheets from Lang-Cre$^-$*Stat5*$^{fl/fl}$ (Lang-Cre$^-$5$^{fl/fl}$) and Lang-Cre$^+$*Stat5*$^{fl/fl}$ (Lang-Cre$^+$5$^{fl/fl}$) mouse ears. Scale bar, 100 μm. (**b**) Expression of CD207 (langerin) and CD11b in MHCII$^+$ cells from the epidermis and dermis of Lang-Cre$^-$*Stat5*$^{fl/fl}$ and Lang-Cre$^+$*Stat5*$^{fl/fl}$ mice. Numbers adjacent to outlined areas indicate percent cells in each. (**c**) Change in ear thickness in wild-type (BALB/c control), Lang-Cre$^-$*Stat5*$^{fl/fl}$ and Lang-Cre$^+$*Stat5*$^{fl/fl}$ mice sensitized on day 0 with 0.5% FITC (on the abdomen), followed by measurement of baseline ear thickness on day 6, then challenge with vehicle or FITC and analysis 24 h after challenge. (**d**) IL-4 mRNA in ear tissue excised and processed 24 h after challenge as in **c** (presented as in **Fig. 1c**). Data are representative of three experiments with five mice per group (**a**), six independent experiments with three mice per group (**b**), three experiments with three to four mice per group (**c**) or three independent experiments with three to four mice per group (**d**; error bars (**c**,**d**), s.e.m.).

© 2013 Nature America, Inc. All rights reserved.

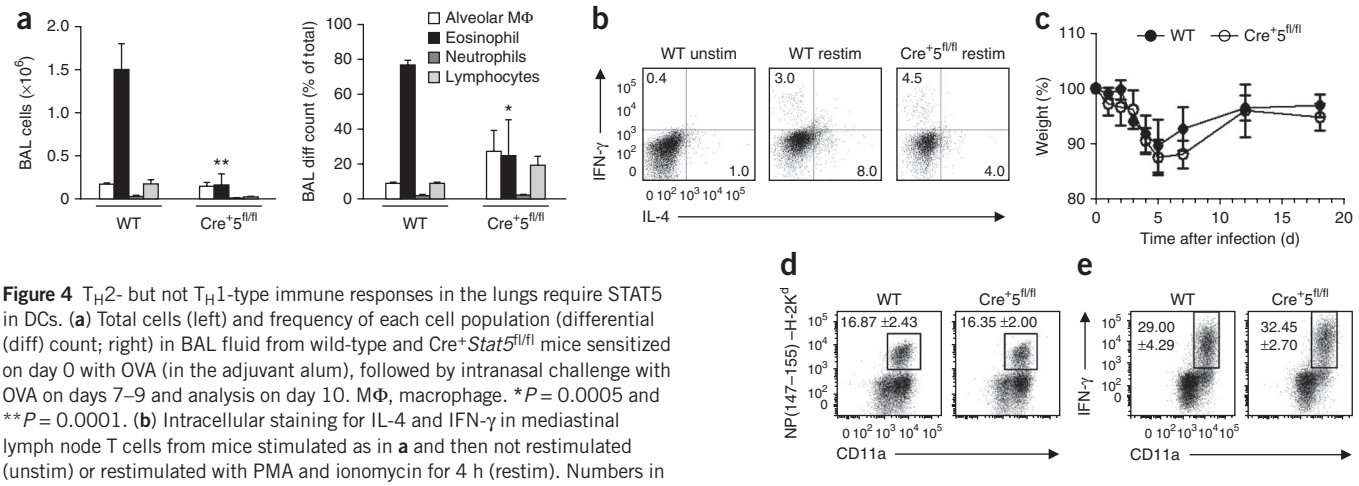

Figure 4 T_H2- but not T_H1-type immune responses in the lungs require STAT5 in DCs. (**a**) Total cells (left) and frequency of each cell population (differential (diff) count; right) in BAL fluid from wild-type and Cre$^+$*Stat5*$^{fl/fl}$ mice sensitized on day 0 with OVA (in the adjuvant alum), followed by intranasal challenge with OVA on days 7–9 and analysis on day 10. MΦ, macrophage. $*P = 0.0005$ and $**P = 0.0001$. (**b**) Intracellular staining for IL-4 and IFN-γ in mediastinal lymph node T cells from mice stimulated as in **a** and then not restimulated (unstim) or restimulated with PMA and ionomycin for 4 h (restim). Numbers in quadrants indicate percent IFN-γ$^+$IL-4$^-$ cells (top left) or IFN-γ$^-$IL-4$^+$ cells (bottom right). (**c**) Weight loss in wild-type and Cre$^+$*Stat5*$^{fl/fl}$ mice infected intranasally with influenza A/Aichi/68 (H3N2; 5×10^3 half-maximal tissue culture infectious doses). (**d**) Antigen-specific CD8$^+$ T cell response on day 8 after infection as in **c**, analyzed with a tetramer of nucleoprotein amino acids 147–155 and H-2K^d (NP(147–155)–H-2K^d). Numbers adjacent to outlined areas indicate percent tetramer-positive CD11a$^+$ (antigen-specific) cells (± s.e.m.). (**e**) IFN-γ production by influenza-stimulated CD4$^+$ T cells (from mice as in **d**) after *in vitro* restimulation with PMA and ionomycin. Numbers adjacent to outlined areas indicate percent IFN-γ$^+$CD11a$^+$ cells (± s.e.m.). Data are representative of two experiments with three mice in each (**a**; average and s.e.m.), two experiments (**b**) or two experiments with five mice per group (**c**–**e**; error bars (**c**), s.e.m.).

© 2013 Nature America, Inc. All rights reserved.

similar to Cre$^+$*Stat5*$^{fl/fl}$ mice (**Fig. 4c**). We saw no difference in total cell numbers in BAL fluid, mediastinal lymph nodes or lungs, as well as no difference in the frequency or number of CD4$^+$ T cells and CD8$^+$ T cells present in these sites at day 8 (data not shown). We found that the immunodominant lung CD8$^+$ T cell response was similar in wild-type and Cre$^+$*Stat5*$^{fl/fl}$ mice (**Fig. 4d**). We noted no difference in the size of the total memory-activated CD8$^+$ T cell compartment (CD44^{hi} CD11a^{hi}) in these mice (data not shown). Similar to the response of lung CD8$^+$ T cells to a tetramer of nucleoprotein amino acids 147–155 and H-2K^d, the number of lung CD4$^+$ T cells able to produce IFN-γ after restimulation *in vitro* with the phorbol ester PMA and ionomycin was similar in wild-type and Cre$^+$*Stat5*$^{fl/fl}$ mice (**Fig. 4e**). Thus, the T_H1 and cytolytic T cell response to influenza A virus seemed intact in Cre$^+$*Stat5*$^{fl/fl}$ mice. Together these results suggested that DCs required STAT5 for the development and promotion of T_H2 responses in the lungs, whereas T_H1 responses were independent of STAT5.

Lack of *in vivo* responses to TSLP in Cre$^+$*Stat5*$^{fl/fl}$ mice

As DC development was unperturbed in Cre$^+$*Stat5*$^{fl/fl}$ mice, we hypothesized that during a T_H2 response, STAT5-inducing cytokines would be critical for DC activation. We assessed the expression of mRNA encoding three STAT5-activating cytokines 24 h after exposure to FITC-DBP[19] (**Supplementary Fig. 3a**). The fourfold greater abundance of TSLP mRNA we noted after such exposure (**Supplementary Fig. 3a**) was consistent with the lack of an inflammatory response to sensitization and challenge with FITC-DBP in TSLPR-deficient mice[23]. Thus, in both skin and lung T_H2 antigen-driven models tested, the absence of STAT5 in DCs was phenocopy of the absence of TSLPR, which suggested that DCs were the *in vivo* target of TSLP.

To assess that hypothesis directly, we used a model of acute airway inflammation by intranasal administration of TSLP and antigen, which led to T_H2 airway inflammation[29] (**Supplementary Fig. 4a**). As seen in TSLPR-deficient mice, Cre$^+$*Stat5*$^{fl/fl}$ mice had no substantial increase in either BAL fluid cell count or recruitment of eosinophils to the bronchoalveolar space after the administration of TSLP and antigen (**Supplementary Fig. 4a**,**b**). Analysis of intracellular cytokine signaling of CD4$^+$ T cells from mediastinal lymph nodes showed that Cre$^+$*Stat5*$^{fl/fl}$ CD4$^+$ T cells had less IL-4 and IL-13 than did wild-type CD4$^+$ T cells (**Supplementary Fig. 4c**). Expression of mRNA encoding CCL17 and IL-4, as well as the concentration of immunoglobulin E in serum, was much lower in Cre$^+$*Stat5*$^{fl/fl}$ lungs than in wild-type lungs (**Supplementary Fig. 4d**,**e**). Each of these findings further supported our hypothesis that TSLP activated STAT5 in DCs in both the skin and lungs to promote T_H2 immunity.

STAT proteins in TSLP-mediated DC maturation

Published work has shown that bone marrow–derived DCs generated either by GM-CSF (GM-DCs) or by Flt3L (FL-DCs) respond to TSLP by upregulating their expression of the costimulatory molecules CD80, CD86 and OX40L and enhancing their production of the chemokine CCL17 (refs. 28,30). We left whole FL-DC cultures untreated or treated them for 96 h with TSLP. There was no change in expression of MHC class II, but surface expression of CD80, CD86 and OX40L was higher in TSLP-treated B220$^-$CD11c$^+$CD11b^{hi}CD24^{int} FL-DCs (FL-CD11b-DCs), whereas TSLP had no effect on B220$^+$CD11c$^+$ Flt3L-induced pDCs (FL-pDCs) or B220$^-$CD11c$^+$CD11b$^+$CD24^{hi} FL-DCs (FL-CD24-DCs)(**Supplementary Fig. 5a**). Time-course analysis showed maximum expression of CD80 and CD86 at 48 h, whereas OX40L expression peaked at 72 h, similar to its expression in human peripheral blood CD11c$^+$ DCs[31]. Treatment of GM-DCs with TSLP similarly led to higher expression of CD86 and OX40L (**Supplementary Fig. 5b**). To determine whether TSLP signaling in the FL-DCs mimicked that in the primary DC subsets they represented, we assessed the effect of TSLP on splenic pDCs, CD4$^+$ DCs and CD8$^+$ DCs *ex vivo*. Similar to FL-CD11b-DCs, only CD4$^+$ splenic DCs had much higher expression of CD80 and CD86 in response to TSLP (**Supplementary Fig. 5c**). However, this was more transient in these cells than in the FL-CD11b-DCs, as expression of CD80 and CD86 was higher at 24 h but was not much higher at 48 h after treatment with TSLP (data not shown). These data suggested that TSLP exerted these effects on specific DC subsets.

TSLP-induced Jak-STAT5 signaling in DCs

Published studies have found that TSLP can activate Jak1 and Jak2 in human DCs[10,11]. We treated the three FL-DC populations noted above for 5 min with TSLP, IL-7 (which activates Jak1) or

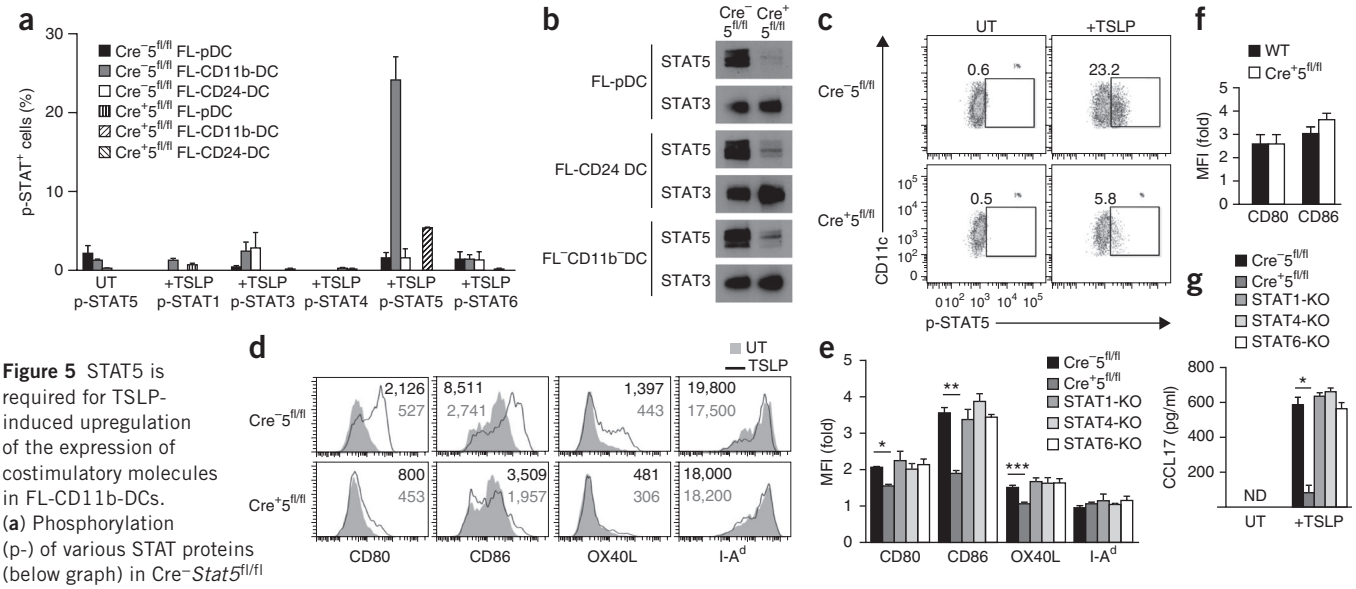

Figure 5 STAT5 is required for TSLP-induced upregulation of the expression of costimulatory molecules in FL-CD11b-DCs. (**a**) Phosphorylation (p-) of various STAT proteins (below graph) in Cre^{-}*Stat5*$^{fl/fl}$ and Cre^{+}*Stat5*$^{fl/fl}$ FL-pDCs, FL-CD11b-DCs and FL-CD24-DCs left untreated (UT) or incubated for 15 min with TSLP (50 ng/ml; +TSLP), assessed by flow cytometry. (**b**) Immunoblot analysis of total STAT5 and STAT3 in FL-DC populations. (**c**) Phosphorylation-specific flow cytometry of Cre^{-}*Stat5*$^{fl/fl}$ and Cre^{+}*Stat5*$^{fl/fl}$ FL-CD11b-DCs treated as in **a**. Numbers above outlined areas indicate percent CD11c^{+} cells with phosphorylated STAT5. (**d**) Expression of costimulatory molecules in untreated and TSLP-treated FL-CD11b-DCs. Numbers in plots indicate mean fluorescence intensity (colors match key). (**e**) Expression of costimulatory molecules in TSLP-treated FL-CD11b-DCs from Cre^{-}*Stat5*$^{fl/fl}$, Cre^{+}*Stat5*$^{fl/fl}$, STAT1-deficient (STAT1-KO), STAT4-deficient (STAT4-KO) and STAT6-deficient (STAT6-KO) bone marrow, presented relative to that in untreated DCs. $*P = 0.01$, $**P = 0.0005$ and $***P = 0.05$ (Student's *t*-test). (**f**) Expression of CD80 and CD86 in wild-type and Cre^{+}*Stat5*$^{fl/fl}$ FL-CD11b-DCs after stimulation with lipopolysaccharide, presented relative to that before stimulation. (**g**) CCL17 in untreated and TSLP-treated FL-CD11b-DCs (as in **e**). $*P = 0.00003$ (Student's *t*-test). Data are from three independent experiments (**a**), three experiments (**b**–**d**), four independent experiments (**e**), two experiments (**f**) or six experiments (**g**; error bars (**a**,**e**–**g**), s.e.m.; triplicates of each sample in each experiment in **a**,**e**,**f**,**g**).

© 2013 Nature America, Inc. All rights reserved.

IL-6 (which activates Jak2) and found that this led to the activation of both Jak1 and Jak2 in FL-CD11b-DCs but not in FL-pDCs or FL-CD24-DCs (**Supplementary Fig. 6a** and data not shown). To directly assess the role of Jak2, we generated FL-DCs from *Jak2*$^{fl/fl}$ mice and infected them with a retrovirus expressing Cre recombinase with a green fluorescent protein (GFP) marker to delete *Jak2*. For these experiments we used uninfected *Jak2*$^{fl/fl}$ FL-CD11b-DCs and retrovirus-infected *Jak2*$^{fl/fl}$ FL-CD11b-DCs sorted into GFP^{-} and GFP^{+} populations and stimulated the cells with TSLP, IL-7 or IL-4. We used CCL17 expression as a 'readout' of TSLP signaling, as the gene encoding CCL17 is a direct target of TSLP[28] (M.K. and S.F.Z., data not shown). GFP^{+} FL-CD11b-DCs stimulated with IL-7 or IL-4 had 50% less CCL17 production than did GFP^{-} and wild-type (control) cells, whereas lack of Jak2 led to 90% less CCL17 production than that in the control cells after treatment with TSLP (**Supplementary Fig. 6b**). In addition, lack of Jak3 had no effect on the phosphorylation of STAT5 after treatment with TSLP relative to that in wild-type FL-CD11b-DCs (data not shown). These data showed that mouse DCs were able to use Jak1 and Jak2 to propagate TSLP signals.

In human myeloid DCs, TSLP has been shown to activate STAT1, STAT3, STAT4, STAT5 and STAT6, although the contributions of individual STAT proteins to the activation of DCs are still unclear[10,11,32]. We assessed the phosphorylation of STAT proteins in all FL-DC populations and, as expected, treatment of FL-DCs with TSLP led to phosphorylated STAT5 only in FL-CD11b-DCs (**Fig. 5a**), although FL-pDCs and FL-CD24-DCs were able to activate STAT1, STAT3, STAT5 and STAT6 in the presence of IFN-α, GM-CSF, GM-CSF and IL-4, respectively (data not shown). We also measured the abundance of the signaling inhibitors SOCS1, SOCS2 and SOCS3 in all three FL-DC populations to determine whether differences in SOCS expression could account for the absence of Jak-STAT signaling in FL-pDCs and FL-CD24-DCs. The expression of SOCS1, SOCS2 and SOCS3 protein was similar in all three FL-DC populations (data not shown). Because STAT5 mediates TSLP-dependent proliferation and the transcription of target genes in many cell lines, we assessed the requirement for STAT5 in TSLP-driven DC maturation[10,12,14]. We confirmed that STAT5 was dispensable for the development of FL-DCs and was efficient in all FL-DC populations[5] (**Fig. 5b**,**c** and data not shown). The lack of STAT5 in FL-CD11b-DCs correlated with less TSLP-induced upregulation of the expression of CD80, CD86 and OX40L (**Fig. 5d**). The residual upregulation of the expression of costimulatory molecules was not due to compensatory upregulation of STAT proteins, as Cre^{+}*Stat5*$^{fl/fl}$ FL-DCs did not have more phosphorylation of STAT1, STAT3, STAT4 or STAT6 than that in Cre^{-}*Stat5*$^{fl/fl}$ FL-DCs (**Fig. 5a**). The absence of STAT1, STAT4, STAT5 or STAT6 did not affect the generation of the three FL-DC subsets (data not shown). Thus, only loss of STAT5 affected upregulation of the expression of CD80, CD86 and OX40L in response to TSLP (**Fig. 5e**). The loss of upregulation of the expression of coreceptors was not due to a developmental defect in Cre^{+}*Stat5*$^{fl/fl}$ DCs, as lipopolysaccharide induced similar expression of CD80 and CD86 in Cre^{+}*Stat5*$^{fl/fl}$ and Cre^{-}*Stat5*$^{fl/fl}$ FL-CD11b-DCs (**Fig. 5f**).

To determine which STAT protein controlled CCL17 production in response to TSLP, we obtained a mouse strain with sequence encoding GFP inserted into the endogenous *Ccl17* locus[33]. As expected, untreated FL-DCs heterozygous for that transgene did not produce CCL17, whereas stimulation with TSLP led to the detection of GFP^{+}CD11c^{+} FL-DCs, and the GFP was confined to the FL-CD11b-DC population (data not shown). Cells lacking STAT5 had much less CCL17 production after treatment with TSLP than did DCs lacking STAT1, STAT4 or STAT6, which had no defect in CCL17 production (**Fig. 5g**). Thus, the TSLP-induced production of CCL17 in mouse

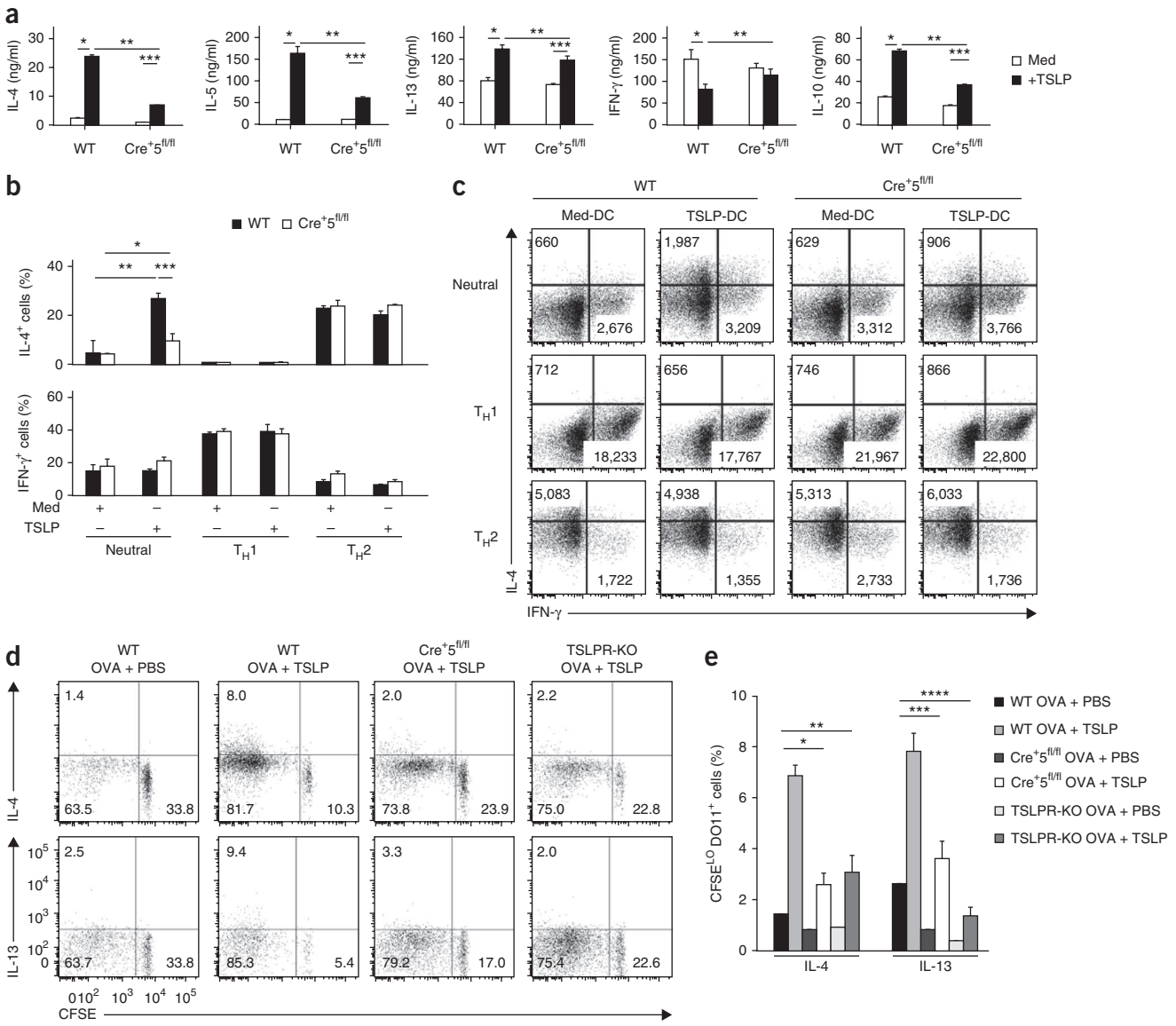

Figure 6 TSLP-induced STAT5 in DCs is required for the T_H2 differentiation of CD4+ T cells. (**a**) Enzyme-linked immunosorbent assay of T_H2 cytokines (vertical axes) in DO11.10 CD4+ T cells cultured for 5 d with OVA(323-339)-pulsed (0.01 μM) Cre−*Stat5*$^{fl/fl}$ and Cre+*Stat5*$^{fl/fl}$ FL-CD11b-DCs that were given no pretreatment (Med) or were pretreated overnight with TSLP (+TSLP), followed by extensive washing for removal of residual TSLP before coculture with T cells. $*P < 0.0005$, $**P < 0.005$ and $***P < 0.05$ (one-way ANOVA). (**b**) Frequency of IL-4+ or IFN-γ+ CD4+ T cells cultured with FL-CD11b-DCs as in **a** in neutral or T_H1- or T_H2-polarizing conditions. $*P < 0.0005$, $**P < 0.005$ and $***P < 0.05$ (one-way ANOVA). (**c**) Flow cytometry of CD4+ T cells as in **b**. Numbers in plots indicate average mean fluorescence intensity for IL-4 (top left) and IFN-γ (bottom right). (**d**) Intracellular cytokine staining of IL-13 and IL-4 and CFSE dilution of cells from skin-draining lymph nodes of wild-type, Cre+*Stat5*$^{fl/fl}$ and TSLPR-deficient (TSLPR-KO) mice given intravenous injection of CFSE-labeled naive DO11.10 CD4+ T cells, followed by intradermal injection of OVA with PBS alone (OVA + PBS) or with TSLP in PBS (OVA + TSLP) and, 7 d later, restimulation of pooled skin-draining lymph nodes with plate-bound monoclonal antibody to CD3 and to CD28, in the presence of monensin, then analysis by flow cytometry. Numbers in quadrants indicate percent cells in each. (**e**) Frequency of IL-4+ or IL-13+ CFSE^{lo} DO11.10 T cells in **d**. $*P = 0.002$, $**P = 0.003$, $***P = 0.001$ and $****P = 0.0003$. Data are representative of three experiments (**a**–**c**), two independent experiments with four mice per group (**d**) or two experiments (**e**; error bars (**a**,**b**,**e**), s.e.m.).

DCs was STAT6 independent. Together these data showed that TSLP activated STAT5 in FL-CD11b-DCs and that activation of STAT5 was required for complete upregulation of the expression of costimulatory molecules and enhanced CCL17 production by FL-CD11b-DCs.

STAT5 activation by TSLP promotes T_H2 signals in DCs

The cumulative effect of TSLP-induced upregulation of the expression of costimulatory molecules and enhanced chemokine production on DCs is the inflammatory T_H2 phenotype adopted by CD4+ T cells primed by such DCs[20]. To determine whether DC-specific STAT5 is required for that process, we cultured wild-type and Cre+*Stat5*$^{fl/fl}$ FL-CD11b-DCs overnight with TSLP, then pulsed the cells with OVA peptide and cultured them together with naive DO11.10 CD4+ T cells (which have transgenic expression of an OVA-specific T cell antigen receptor) labeled with the cytosolic dye CFSE. Untreated DCs generated from wild-type and Cre+*Stat5*$^{fl/fl}$ bone marrow produced similar CFSE dilution profiles in activated CD4+ T cells, whereas wild-type DCs promoted enhanced proliferation of CD4+ T cells

© 2013 Nature America, Inc. All rights reserved.

after TSLP treatment, but STAT5-deficient DCs did not (data not shown). Accordingly, the abundance of T_H2 cytokines was significantly lower in $CD4^+$ T cells cultured with TSLP-treated Cre^+*Stat5*$^{fl/fl}$ DCs than in those cultured with TSLP-treated wild-type DCs (**Fig. 6a**). Furthermore, only wild-type TSLP-treated DCs were able to diminish the production of IFN-γ by the activated $CD4^+$ T cells. We obtained similar results with TSLPR-deficient DO11.10 T cells (data not shown). Finally, we assessed the ability of Cre^+*Stat5*$^{fl/fl}$ and wild-type DCs to promote the expression of IFN-γ and IL-4 by $CD4^+$ T cells in neutral, T_H1- and T_H2-skewing conditions. When the DCs were not pretreated with TSLP, similar numbers of IFN-γ^+ and IL-4^+ $CD4^+$ T cells were generated under neutral, T_H1- and T_H2-skewing conditions (**Fig. 6b**,**c**). These data showed that FL-CD11b-DCs that lacked STAT5 were able to generate both T_H1 and T_H2 cells under the appropriate conditions and that the defect in the activation of T_H2 cells occurred only in the absence of STAT5 in TSLP-treated DCs.

To assess the T cell–stimulatory ability of STAT5-deficient DCs *in vivo*, we transferred CFSE-labeled DO11.10 $CD4^+$ T cells into wild-type, Cre^+*Stat5*$^{fl/fl}$ and TSLPR-deficient hosts. Intradermal injection of OVA in PBS led to dilution of CFSE and detectable numbers of IL-4^+ and IL-13^+ $CFSE^{lo}$ $CD4^+$ T cells in all three hosts (**Fig. 6d**,**e**), which showed that dermal DCs lacking STAT5 or TSLPR were able to migrate, process antigen and present antigen to naive $CD4^+$ T cells. Intradermal injection of OVA plus TSLP led to enhanced T cell proliferation and production of IL-4 and IL-13 in wild-type hosts (**Fig. 6d**,**e**). That enhancement of the production of T_H2 cytokines in the presence of antigen and TSLP was absent in Cre^+*Stat5*$^{fl/fl}$ and TSLPR-deficient hosts. Thus, consistent with the *in vitro* data, DCs required STAT5 *in vivo* for TSLP-mediated T_H2 differentiation.

DISCUSSION

We were unable to determine from our data whether STAT5 was critical for DC development, as CD11c is expressed late in development[34]. However, it was apparent that STAT5 was dispensable for DC homeostasis. That finding differed from published work showing that STAT5 deficiency leads to fewer cDCs[5]. In that study, fetal liver cells from wild-type and STAT5-deficient mice were used to reconstitute lethally irradiated hosts; those reconstituted mice were immunodeficient, which affected splenic architecture and the number of DCs[5]. In our studies here, STAT5 was deleted only in cells that expressed CD11c, and the only discernible difference we found was less cellularity of the lymphoid and myeloid lineage in lymph nodes. When STAT5 deletion was restricted to LCs, lymph node cellularity remained at the amount in wild-type mice, which suggested that the defect arose only when dermal and/or lymph node–resident DCs lacked STAT5. Therefore, we believe that our model provides a more accurate reflection of the role of STAT5 in DC in homeostasis and survival than do published studies using germline knockout of *Stat5* in DCs, and that DCs do not require STAT5 for their homeostasis.

Our data were both similar to and distinct from a published study showing that after deletion of STAT3 in DCs via the CD11c-Cre system, cDC development is largely unaffected[23]. However, that study found 50% fewer splenic and bone marrow pDCs, whereas we did not. The main difference between the two sets of mice is the development of lymphadenopathy and ileocolitis in Cre^+*Stat3*$^{fl/fl}$ mice[23]. That phenotype was attributed to an enhanced activation state of the DCs in those mice. Our analysis of aged Cre^+*Stat5*$^{fl/fl}$ mice has not shown any obvious indication of spontaneous inflammation (data not shown). These data suggest different cell-intrinsic roles for STAT3 and STAT5 in DCs homeostasis after deletion mediated by the CD11c-Cre system.

We found specificity for the deficit in DCs from Cre^+Stat*Stat5*$^{fl/fl}$ mice. In general, these mice had no overt signs of pathology, which suggested that their DC function was normal, as either constitutive or conditional ablation of DCs leads to systemic inflammation and autoimmunity[35,36]. In addition, we found that DCs from these mice were able to promote both T_H1 and T_H2 differentiation in an antigen-driven *in vitro* system. In addition, the mice retained normal T_H1 responses to DNFB and infection with influenza virus, which demonstrated the maintenance of DC function, including antigen acquisition, trafficking, activation of T cells and cytokine production.

An unexpected finding of our study was the specificity of the defect for T_H2 responses *in vivo* in the absence of STAT5 in DCs, as shown by a lack of response to the T_H2 hapten FITC and T_H2-type allergic responses in the lung. The requirement for STAT5 in DCs was restricted to dermal DCs, as Lang-Cre^+*Stat5*$^{fl/fl}$ mice responded normally to FITC-DBP. To determine the cause of this defect, we assessed the production of STAT5-activating cytokines and found considerable upregulation of TSLP expression after sensitization with FITC (T_H2 hapten) but not after sensitization with DNFB (T_H1 hapten)[19]. In a wide variety of model systems, higher expression of TSLP leads to the induction of T_H2 inflammation. TSLP has a critical role in driving antigen-induced airway inflammation in the mouse[17,28,29]. High expression of TSLP in the skin leads to the development of an atopic dermitis–like disease[37–40]. Furthermore, TSLPR-deficient mice have a considerably diminished response in a T_H2 model of CHS[19]. We have extended those results to show that in the presence of antigen and TSLP alone, STAT5 was required in DCs for the development of the response. Those data, along with the much lower response of Cre^+*Stat5*$^{fl/fl}$ mice in the OVA-induced allergy model, are consistent with the proposal that STAT5 is a critical downstream mediator of TSLPR signals in DCs.

As noted above, human myeloid DCs activated by TSLP have phosphorylation of various STAT proteins[11]. Only STAT5 was phosphorylated after stimulation with TSLP, and this was restricted to FL-CD11b-DCs. STAT5 seemed to control all of the TSLP-mediated effects, as the absence of STAT5 led to upregulation of the expression of CD80, CD86 and OX40L. Unlike CCL17 production in human DCs, the production of CCL17 after TSLP stimulation in mouse DCs required only STAT5.

It is unclear why the FL-CD24-DC and FL-pDC subsets did not activate STAT5 in response to TSLP, as we have found similar amounts of IL-7Rα and TSLPR on the surface of these DCs (data not shown). One possibility is the presence of as-yet-unidentified inhibitory molecules, as we found similar expression of SOCS1, SOCS2 and SOCS3 protein in all three FL-DC subsets (data not shown). To understand the specificity of the effect of TSLP on specific DC subsets (FL-CD11b-DCs and GM-DCs), we did microarray analysis of wild-type, Cre^+*Stat5*$^{fl/fl}$ and TSLPR-deficient FL-DCs. We found that TSLP did indeed cause changes in many targets in the FL-pDC and FL-CD24-DC subsets (data not shown). We also found that for FL-CD11b-DCs, the absence of STAT5 did not affect approximately 15% of the TSLP-responsive genes (data not shown), which suggests that other signaling pathways are activated downstream of the TSLPR.

The importance of TSLP in the initiation and progression of allergic disease is becoming clear. Less clear is the identity of the key TSLP-responsive cells at sites of disease and the nature of the signaling pathways used by those cells to respond to the cytokine. Collectively, our data suggest a model by which STAT5 specifically mediates TSLP responses in DCs after antigen acquisition in the periphery.

© 2013 Nature America, Inc. All rights reserved.

METHODS

Methods and any associated references are available in the online version of the paper.

Note: Supplementary information is available in the online version of the paper.

ACKNOWLEDGMENTS

We thank D. Kaplan (University of Minnesota) for langerin-Cre mice; I. Förster (University of Bonn) for mice with a transgene encoding GFP in the *Ccl17* locus; T. Nakayama (Chiba University) for pMX-Cre-IRES-GFP; D. Rawlings and H. Kerns (Seattle Children's Research Institute) for Btk- and Tec-deficient bone marrow; J. Hamerman and D. Campbell for discussions of the manuscript; S. Ma and W. Xu for technical support; and M. Warren and S. McCarty for administrative support. Supported by the US National Institutes of Health (R01-AI068731, R01-AR056113, R01-AR055695 and P01-HL098067 to S.F.Z., and 5T32AI007411-19 to B.D.B.).

AUTHOR CONTRIBUTIONS

B.D.B. and M.K. did most of the experiments and wrote the manuscript, with help from S.F.Z.; K.S., K.-U.W., B.R. and L.H. provided mouse strains and expertise; R.P.L. collaborated on the CHS studies; T.A.S. did the influenza infections and analyzed the response to infection; K.D. provided help with bioinformatics; and S.F.Z. supervised the work.

COMPETING FINANCIAL INTERESTS

The authors declare no competing financial interests.

Reprints and permissions information is available online at http://www.nature.com/reprints/index.html.

1. Shortman, K. & Naik, S.H. Steady-state and inflammatory dendritic-cell development. *Nat. Rev. Immunol.* **7**, 19–30 (2007).
2. McKenna, H.J. *et al.* Mice lacking flt3 ligand have deficient hematopoiesis affecting hematopoietic progenitor cells, dendritic cells, and natural killer cells. *Blood* **95**, 3489–3497 (2000).
3. Laouar, Y., Welte, T., Fu, X.Y. & Flavell, R.A. STAT3 is required for Flt3L-dependent dendritic cell differentiation. *Immunity* **19**, 903–912 (2003).
4. Onai, N., Obata-Onai, A., Tussiwand, R., Lanzavecchia, A. & Manz, M.G. Activation of the Flt3 signal transduction cascade rescues and enhances type I interferon-producing and dendritic cell development. *J. Exp. Med.* **203**, 227–238 (2006).
5. Esashi, E. *et al.* The signal transducer STAT5 inhibits plasmacytoid dendritic cell development by suppressing transcription factor IRF8. *Immunity* **28**, 509–520 (2008).
6. Schiavoni, G. *et al.* ICSBP is essential for the development of mouse type I interferon-producing cells and for the generation and activation of CD8α^+ dendritic cells. *J. Exp. Med.* **196**, 1415–1425 (2002).
7. Zenke, M. & Hieronymus, T. Towards an understanding of the transcription factor network of dendritic cell development. *Trends Immunol.* **27**, 140–145 (2006).
8. Ziegler, S.F. & Artis, D. Sensing the outside world: TSLP regulates barrier immunity. *Nat. Immunol.* **11**, 289–293 (2010).
9. Liu, Y.J. *et al.* TSLP: an epithelial cell cytokine that regulates T cell differentiation by conditioning dendritic cell maturation. *Annu. Rev. Immunol.* **25**, 193–219 (2007).
10. Rochman, Y. *et al.* Thymic stromal lymphopoietin-mediated STAT5 phosphorylation via kinases JAK1 and JAK2 reveals a key difference from IL-7-induced signaling. *Proc. Natl. Acad. Sci. USA* **107**, 19455–19460 (2010).
11. Arima, K. *et al.* Distinct signal codes generate dendritic cell functional plasticity. *Sci. Signal.* **3**, ra4 (2010).
12. Isaksen, D.E. *et al.* Requirement for stat5 in thymic stromal lymphopoietin-mediated signal transduction. *J. Immunol.* **163**, 5971–5977 (1999).
13. Levin, S.D. *et al.* Thymic stromal lymphopoietin: a cytokine that promotes the development of IgM$^+$ B cells in vitro and signals via a novel mechanism. *J. Immunol.* **162**, 677–683 (1999).
14. Isaksen, D.E. *et al.* Uncoupling of proliferation and Stat5 activation in thymic stromal lymphopoietin-mediated signal transduction. *J. Immunol.* **168**, 3288–3294 (2002).
15. Rochman, Y., Spolski, R. & Leonard, W.J. New insights into the regulation of T cells by γ_c family cytokines. *Nat. Rev. Immunol.* **9**, 480–490 (2009).
16. Kitajima, M., Lee, H.C., Nakayama, T. & Ziegler, S.F. TSLP enhances the function of helper type 2 cells. *Eur. J. Immunol.* **41**, 1862–1871 (2011).
17. Al-Shami, A., Spolski, R., Kelly, J., Keane-Myers, A. & Leonard, W.J. A role for TSLP in the development of inflammation in an asthma model. *J. Exp. Med.* **202**, 829–839 (2005).
18. He, R. *et al.* TSLP acts on infiltrating effector T cells to drive allergic skin inflammation. *Proc. Natl. Acad. Sci. USA* **105**, 11875–11880 (2008).
19. Larson, R.P. *et al.* Dibutyl phthalate-induced thymic stromal lymphopoietin is required for th2 contact hypersensitivity responses. *J. Immunol.* **184**, 2974–2984 (2010).
20. Soumelis, V. *et al.* Human epithelial cells trigger dendritic cell mediated allergic inflammation by producing TSLP. *Nat. Immunol.* **3**, 673–680 (2002).
21. Henri, S. *et al.* Disentangling the complexity of the skin dendritic cell network. *Immunol. Cell Biol.* **88**, 366–375 (2010).
22. Merad, M. & Manz, M.G. Dendritic cell homeostasis. *Blood* **113**, 3418–3427 (2009).
23. Melillo, J.A. *et al.* Dendritic cell (DC)-specific targeting reveals Stat3 as a negative regulator of DC function. *J. Immunol.* **184**, 2638–2645 (2010).
24. Gorbachev, A.V. & Fairchild, R.L. Induction and regulation of T-cell priming for contact hypersensitivity. *Crit. Rev. Immunol.* **21**, 451–472 (2001).
25. Takeshita, K., Yamasaki, T., Akira, S., Gantner, F. & Bacon, K.B. Essential role of MHC II-independent CD4$^+$ T cells, IL-4, and STAT6 in contact hypesensitivity induced by fluorscein isothiocyanate in the mouse. *Int. Immunol.* **16**, 685–695 (2004).
26. Dearman, R.J. & Kimber, I. Role of CD4$^+$ T helper 2-type cells in cutaneous inflammatory responses induced by flourscein isothiocyanate. *Immunology* **101**, 442–451 (2000).
27. Bobr, A. *et al.* Acute ablation of Langerhans cells enhances skin immune responses. *J. Immunol.* **185**, 4724–4728 (2010).
28. Zhou, B. *et al.* Thymic stromal lymphopoietin as a key initiator of allergic airway inflammation in mice. *Nat. Immunol.* **6**, 1047–1053 (2005).
29. Headley, M.B. *et al.* TSLP conditions the lung immune environment for the generation of pathogenic innate and antigen-specific adaptive immune responses. *J. Immunol.* **182**, 1641–1647 (2009).
30. Taylor, B.C. *et al.* TSLP regulates intestinal immunity and inflammation in mouse models of helminth infection and colitis. *J. Exp. Med.* **206**, 655–667 (2009).
31. Ito, T. *et al.* TSLP-activated dendritic cells induce an inflammatory T helper type 2 cell response through OX40 ligand. *J. Exp. Med.* **202**, 1213–1223 (2005).
32. Ziegler, S.F. The role of thymic stromal lymphopoietin (TSLP) in allergic disorders. *Curr. Opin. Immunol.* **22**, 795–799 (2010).
33. Alferink, J. *et al.* Compartmentalized production of CCL17 *in vivo*: Strong inducibility in peripheral dendritic cells contrasts selective absence from the spleen. *J. Exp. Med.* **197**, 585–599 (2003).
34. Caton, M.L., Smith-Raska, M.R. & Reizis, B. Notch-RBP-J signaling controls the homeostasis of CD8- dendritic cells in the spleen. *J. Exp. Med.* **204**, 1653–1664 (2007).
35. Birnberg, T. *et al.* Lack of conventional dendritic cells is compatible with normal development and T cell homeostasis, but causes myeloid proliferative syndrome. *Immunity* **29**, 986–997 (2008).
36. Ohnmacht, C. *et al.* Constitutive ablation of dendritic cells breaks self-tolerance of CD4 T cells and results in spontaneous fatal autoimmunity. *J. Exp. Med.* **206**, 549–559 (2009).
37. Yoo, J. *et al.* Spontaneous atopic dermatitis in mice expressing an inducible thymic stromal lymphopoietin transgene specifically in the skin. *J. Exp. Med.* **202**, 541–549 (2005).
38. Li, M. *et al.* Topical vitamin D3 and low-calcemic analogs induce thymic stromal lymphopoietin in mouse keratinocytes and trigger an atopic dermatitis. *Proc. Natl. Acad. Sci. USA* **103**, 11736–11741 (2006).
39. Briot, A. *et al.* Kallikrein 5 induces atopic dermatitis-like lesions through PAR2-mediated thymic stromal lymphopoietin expression in Netherton syndrome. *J. Exp. Med.* **206**, 1135–1147 (2009).
40. Dumortier, A. *et al.* Atopic dermatitis-like disease and associated lethal myeloproliferative disorder arise from loss of notch signaling in the murine skin. *PLoS ONE* **5**, e9258 (2010).

© 2013 Nature America, Inc. All rights reserved.

ONLINE METHODS

Animals. Six- to twelve-week-old female BALB/c mice, Jak3-deficient and STAT6-deficient mice were from Taconic Farms and Jackson Laboratory. Mice with sequence encoding red fluorescent protein along with a *lox*P-flanked transcriptional 'stop' sequence inserted into the ubiquitously expressed *Rosa26* locus[41] and with transgenic expression of *Cd11c*-Cre from a bacterial artificial chromosome[34] were backcrossed ten generations onto the BALB/c background and then were crossed with mice with *lox*P-flanked *Stat5* alleles on the BALB/c background[42]. The langerin-Cre mice were provided by D. Kaplan[43]. Mice with *lox*P-flanked *Jak2* alleles were on the BALB/c background. STAT1-deficient mice on the BALB/c background (Taconic) were backcrossed to the BALB/c background for more than ten generations. STAT4-deficient mice on the BALB/c background were from Jackson Laboratory. DO11.10 mice (with transgenic expression of OVA-specific T cell antigen receptor αβ) were from Jackson Laboratory[44]. Mice with a transgene encoding GFP in the *Ccl17* locus on the BALB/c background were from I. Förster[33]. All mice were maintained under pathogen-free conditions. All animal procedures were in accordance with Institutional Animal Care and Use Committee guidelines at the Benaroya Research Institute.

Flow cytometry. In general, 1×10^6 cells were stained with antibodies. For surface staining, the following antibodies were used: phycoerythrin-indotricarbocyanine–conjugated monoclonal antibody (mAb) to CD11c (N418), Alexa Fluor 647–conjugated mAb to CD80 (16-10A1), Pacific blue–conjugated mAb to CD11b (M1/70), FITC-conjugated mAb to B220 (RA306B2), Pacific blue–conjugated mAb to CD3ε (145-2C11), Pacific blue–conjugated mAb to CD19 (1D3), peridinin chlorophyll protein–cyanine 5.5–conjugated mAb to Ly-6C (HK1.4) and Pacific blue–conjugated mAb to Ly-6G (RB6-8C5; all from BioLegend); phycoerythrin-conjugated mAb to IL-7Rα (A7R34), phycoerythrin-conjugated mAb to FcεRα (MAR-1), phycoerythrin-conjugated mAb to CD86 (PO3.1), phycoerythrin-conjugated mAb to OX40L (RM134L), Alexa Fluor 700–conjugated mAb to CD8α (53-6.7), Alexa Fluor 780–conjugated mAb to CD4 (RM4-5), phycoerythrin-conjugated mAb to CD103 (2E7), allophycocyanin-conjugated mAb to F4/80 (BM8), FITC-conjugated mAb to the mouse DO11.10 T cell antigen receptor (KJ1-26), Alexa Fluor 700–conjugated mAb to CD44 (IM7) and allophycocyanin-conjugated streptavidin (all from eBioscience); FITC-conjugated mAb to I-A^d (AMS-32.1) and phycoerythrin-indotricarbocyanine–conjugated mAb to CD11a (2D7; both from BD Bioscience); and biotin-conjugated mAb to TSLPR (22H9 (ref. 14); purified in-house). For intracellular staining, Alexa Fluor 488–conjugated mAb to CD207 (927F301; Dendritics), phycoerythrin-indotricarbocyanine–conjugated mAb to IL-4 (BVD6-24G2; eBioscience) and eFlour 450–conjugated mAb to IFN-γ (XMG1.2; eBioscience) were used. For intracellular staining of phosphorylated STAT proteins, antibody to STAT1 phosphorylated at Tyr701 (4a), antibody to STAT3 phosphorylated at Tyr705 (38/P-STAT3), antibody to STAT4 phosphorylated at Tyr693 (38/p-STAT4), antibody to STAT5 phosphorylated at Tyr694 (47/STAT5(pY694)) and antibody to STAT6 phosphorylated at Tyr641 (J71-773.58.11) were used (all from BD Biosciences). Cells were analyzed on an LSR II with FACSDiva software or on a FACSCalibur with CellQuest Pro software and were sorted at 4 °C on FACSAria II (all from BD Biosciences) and analyzed with FlowJo software (TreeStar).

Bone marrow DC cultures. A modified method was used for bone marrow DC cultures as described[5,45]. Bone marrow cells collected from femurs and tibias were cultured in the presence of 10 ng/ml mouse GM-CSF (granulocyte-macrophage colony-stimulating factor; Peprotech), with half of the medium replenished every other day with fresh GM-CSF, for GM-DCs, or 200 ng/ml human Flt3L (gift from Amgen) for FL-DCs, in RPMI-1640 medium supplemented with 10% FBS, 2-mercaptoethanol, L-glutamine, HEPES, pH7.4, sodium pyruvate, MEM nonessential amino acids, penicillin and streptomycin (complete RPMI). On days 7–9, cells were collected and $CD11c^+$ DCs were positively isolated with micro beads conjugated to mAb to CD11c (N418; Miltenyi Biotech) and a MACS LS column (Miltenyi Biotech) or DC populations were purified by sorting on a FACSAria II (BD). GM-DCs were sorted as $MHCII^{hi}CD11c^{hi}$ cells. FL-DCs were sorted as pDCs ($B220^+CD11c^+$), CD11b-DCs ($B220^-CD11c^+CD11b^{hi}CD24^{int}$) and CD24-DCs ($B220^-CD11c^+CD11b^+CD24^{hi}$). The purity was over 90% (data not shown). Cells were stimulated for various times with medium alone or medium plus 50 ng/ml of TSLP.

Quantitative RT-PCR, DNA deletion and microarray. Total RNA was isolated from cells with a GenElute Mammalian Total RNA Kit (Sigma) or from tissue with TRIzol reagent (Invitrogen), and reverse transcription was done with Superscript II RT according to the manufacturer's protocol (Invitrogen). PCR amplification was done on ABI 7700 Sequence Detector (Applied Biosystems). Quantitative RT-PCR was done as described with primers for *Il4*, *Il17a* and *Ifng*[19,46]. Expression was normalized by the *Gapdh* signal. The primers used were as follows: TSLPR-encoding gene (*Crlf2*; called '*Tslpr*' here) forward, 5′-GAGAGCAATGACGATGAGGAC-3′; *Tslpr* reverse, 5′-GATCTTCCTGCACAGCCAGA-3′; *Il7ra* forward, 5′- GAGAAACTGGTATCAGGATTCCC-3′; *Il7ra* reverse, 5′-GTCTTCAGAGACAGCCAGGA-3′; *Gapdh* forward, 5′-TGCACCACCAACTGCTTAG-3′; *Gapdh* reverse, 5′-GGATGCAGGGATGATGTTC-3′. The *lox*P-flanked *Stat5* alleles and deletion of *Stat5* in germline DNA were detected as described[42]. For microarray, FL-DCs were sorted as CD11b-DCs, CD24-DCs and pDCs, and cells were cultured overnight with medium plus Flt3L (100 ng/ml), then cells were stimulated for 6 h with medium alone or TSLP (50 ng/ml). Total RNA was isolated from cells with an RNeasy mini-kit according to the manufacturer's instructions (Qiagen) and was amplified with Illumina TotalPrep-96 RNA Amplification Kit (Ambion). The resulting cRNA was hybridized to an Illumina MouseWG-6 v2.0 BeadChip (Illumina), followed by scanning on a HiScan SQ according to the manufacturer's protocols (Illumina). An Agilent Bioanalyer 2100 (Agilent Technologies) and a Tecan Infinite M200 pro Nanoquant (Tecan) were used for quality control. Data were normalized and analyzed with R software (R project for statistical computing).

Retroviral vectors and infection. The plasmid pMX-Cre-IRES-GFP was provided by T. Nakayama. The method for the generation of virus supernatant has been described[47]. FL-DCs were infected with viral supernatant in media (at ratio of 1:1) 48 h after start of Flt3L culture by centrifugation (1,800 r.p.m. (750*g*) for 1 h). On the next day, virus was washed from cells and fresh medium containing Flt3L was added. At 5 d after infection, GFP^+ and GFP^- CD11b-DCs were sorted with a FACSAria II (BD). CD11b-DCs were stimulated for 72 h with medium alone or 50 ng/ml TSLP and supernatants were collected for enzyme-linked immunosorbent assay (ELISA) of CCL17.

Immunoprecipitation and immunoblot analysis. FL-CD11b-DCs were stimulated for various times with 50 ng/ml of the appropriate cytokine. Cell extracts were prepared with 150 mM NaCl lysis buffer containing 1% Triton X-100, including complete protease and phosphatase inhibitors (Sigma-Aldrich). Cell extracts were resolved by electrophoresis through 4–12% Bis-Tris NuPage gels (Invitrogen) and were transferred to nitrocellulose membranes (Bio-Rad). The membranes were probed with antibody to Jak1 phosphorylated at Tyr1022 and Tyr1023 (3331), antibody to total Jak1 (6G4), antibody to Jak2 phosphorylated at Tyr1007 and Tyr1008 (3371), antibody to total Jak2 (D2E12), antibody to total STAT3 (124H6), antibody to total STAT5 (9363), antibody to STAT3 phosphorylated at Tyr705 (9131), antibody to STAT5 phosphorylated at Tyr694 (12H2), antibody to total SOCS1 (A156), antibody to total SOCS2 (2779), antibody to total SOCS3 (L210; all from Cell Signaling). Proteins were visualized with horseradish peroxidase–conjugated secondary antibodies (7074 and 7076; Cell Signaling) by ECL detection system (Millipore). For immunoprecipitation, 2×10^7 cells were cultured for 30 min in medium containing 1% serum (to diminish background phosphorylation), and antibody to total Jak1 (6G4) and antibody to total Jak2 (D2E12) were used according to the manufacturer's protocol (Cell Signaling).

***In vitro* $CD4^+$ cell differentiation culture.** FL-CD11b-DCs were sorted, and cells were stimulated for 1 or 2 d with medium or TSLP (50 ng/ml). Cells were washed and then were pulsed for 1 h with OVA(323–339) (0.01 μM). Naive splenic $CD4^+CD62L^+$ T cells (2.5×10^5 cells per ml) from DO11.10 mice were stimulated in the presence of medium- or TSLP-treated CD11b-DCs (5×10^4 cells per ml) in 96-well round-welled plate. Residual TSLP was extensively washed off the DCs before the addition of T cells. For CFSE-dilution assays, $CD4^+$ cells were labeled for 8 min at 37 °C with

© 2013 Nature America, Inc. All rights reserved.

5 μM CFSE (carboxyfluorescein diacetate succinimidyl ester; Invitrogen) before coculture. The following were also added to the culture: for the induction of T_H1 cells, IL-2 (25U/ml; eBioscience), IL-12 (1 ng/ml; eBioscience), antibody to IL-4 (IL-4; 11B11; 1 μg/ml; US National Institutes of Health); T_H2, IL-2 (25 U/ml; eBioscience), IL-4 (10 ng/ml; eBioscience), mAb to IFN-γ (supernatant of hybridoma R4-6A2; 10%; American Type Culture Collection). On day 3, IL-2 was added and cells were maintained with IL-2 until day 5. Cells were collected and washed, and then cells (5×10^4) were stimulated for 2 d with plate-bound mAb to CD3 (6 μg/ml; 2C11) and mAb to CD28 (8 μg/ml; 35.71; both from the University of California, San Francisco). Supernatants were collected and IL-4, IL-5, IL-13 and IFN-γ were measured by ELISA as described[46]. IL-10 was measured with clones JES5-16E3 and JES5-2A5 (eBioscience). For intracellular staining of cytokines, cells were stimulated for 6 h with plate-bound mAb to CD3 and mAb to CD28in the presence of monensin (eBioscience). Intracellular cytokines were stained with a Cytofix/Cytoperm Fixation/Permeabilization Kit according to the manufacturer's protocol (BD Biosciences).

DC isolation. Ears were removed with scissors and split with two pairs of forceps and then were floated (with the dermis side down) for 1 h at 37 °C in dispase (3 mg/ml or 2.4 U/ml, according to the manufacturer's recommendation; Roche). LCs and dermal DCs were isolated for flow cytometry by removal of the epidermis from dermis with two sets of forceps and placement of each (separately) for 30 min at 37 °C in 50 μg/ml Liberase with shaking. Liberated cells were then washed three times in ice cold PBS.

Fluorescence microscopy. Epidermal sheets were separated from the dermal layer by digestion for 1 h at 37 °C in dispase (Roche). The epidermis was washed three times in PBS, fixed for 15 min at −20 °C in ice-cold methanol, washed two times in PBS, and rehydrated for 30 min at room temperature (15–25 °C) in PBS. Nonspecific binding on the epidermis was then blocked with two incubations in 1% BSA and 0.1% Tween-20 in PBS, followed by overnight incubation at 4 °C with FITC-conjugated antibody to MHC class II (AMS-32.1; BD Bioscience) diluted 1:200 in blocking buffer. The epidermis was washed five more times the next day, followed by mounting on glass slides with VECTASHIELD with DAPI (4,6-diamidino-2-phenylindole; Vector Labs) and imaging on a DMIRB inverted microscope.

Intradermal injection. Mice were given intravenous injection of CFSE-labeled naive DO11CD4$^+$ T cells. Then, 4 h later, mice were given intradermal injection (on the shaved back) of 5 μg OVA with or without 5 μg TSLP in PBS. Then, 7 d later, pooled skin-draining lymph nodes were restimulated with PMA and ionomycin for 4 h in the presence of monensin.

CHS. CHS was induced in mice through the use of the hapten FITC or DNFB). FITC was resuspended in acetone and DBP (at a ratio of 1:1) to a concentration of 0.5%. DNFB was diluted to a concentration of 0.5% in acetone and olive oil (at a ratio of 4:1). On day 0, mice were sensitized with 100 μl 0.5% FITC or vehicle (DBP and acetone at a ratio of 1:1) for the FITC model; or with 50 μl 0.5% DNFB or vehicle (4:1 acetone/olive oil) for the DNFB model. On day 6, baseline ear thickness was measured with calipers, followed by challenge of the mice on one ear with 20 μl of 0.5% hapten and vehicle on the contralateral ear. On day 7, 24 h after challenge, ear thickness was measured for calculation of the change in ear thickness. In some experiments, hapten-sensitized mice given intraperitoneal injection of BrdU (5-bromodeoxyuridine) at a dose of 1 mg per day on days 1 through 5.

ELISA. FL-DCs (2×10^5) were stimulated for 3 d with medium alone or medium plus TSLP (50 ng/ml). The abundance of CCL17 was measured with a mouse CCL17 ELISA Kit according to the manufacturer's protocol (R&D Systems).

Infection with influenza virus A, tissue preparation and analysis. Mice were lightly anesthetized with ketamine (100 mg per kg body weight) and xylazine (1 mg per kg body weight) and then intranasally infected with influenza A virus X-31 (A/Aichi/68 (H3N2); 5×10^3 half-maximal tissue culture infectious doses) in 30 μl PBS. At the appropriate times, mice were given lethal intraperitoneal injection of 1 ml of 2.5% Avertin in PBS. Lungs were subjected to BAL five times, each with 1 ml PBS delivered through a tracheal cannula, followed by cardiac perfusion with 10 ml PBS. Cells in BAL fluid were pelleted and then resuspended in RPMI-1640 medium with 5% FCS, HEPES, pH 7.4, penicillin-streptomycin and glutamine. Lung and mediastinal lymph nodes were minced into small pieces and were incubated for 1 h (lungs) or 30 min (mediastinal lymph nodes) at 37 °C under agitation in collagenase buffer (RPMI-1640 medium, 2% FCS, HEPES, pH 7.4, penicillin-streptomycin, glutamine, $CaCl_2$, $MgCl_2$ and collagenase (100 U/ml; Invitrogen)). At the end of the incubation, remaining tissue pieces were crushed through 100-μm nylon mesh filter (BD Biosciences). The resulting mediastinal lymph node cells were pelleted and then were resuspended in RPMI 1640 medium with 5% FCS, HEPES. pH 7.4, penicillin-streptomycin and glutamine, whereas the resulting lung cells were pelleted and then were resuspended in 44% Percoll buffer (GE Life Sciences) and underlaid with 67% Percoll buffer. Percoll gradients were centrifuged at 1,700*g*, and cells at the Percoll gradient interface were extracted and washed and then were resuspended in RPMI-1640 medium, 5% FCS, HEPES, pH 7.4, penicillin-streptomycin and glutamine. For staining, lymphocytes were suspended in flow cytometry buffer (0.2% BSA and 0.1% NaN_3 in PBS) at a concentration of 2×10^6 cells per 50 μl and were stained at 4 °C for 20 min with peridinin chlorophyll protein–cyanine 5.5–conjugated mAb to CD4 (RM4-5; BioLegend), Pacific blue–conjugated mAb to CD8α (53-6.7; BioLegend), Alexa Fluor 700–conjugated mAb to CD44 (IM7; eBioscience) and phycoerythrin-indotricarbocyanine–conjugated mAb to CD11a (2D7; BD Biosciences), then were washed and then fixed with 2% paraformaldehyde in PBS. For tetramer staining, cells were incubated for 1 h at room temperature (15–25 °C) with the tetramer NP(147–155)–H-2K^d (US National Institutes of Health Tetramer Core Facility) and antibodies, then were washed and then fixed in PBS with 2% paraformaldehyde. For *in vitro* T cell–restimulation assays, 2×10^6 cells from lungs were resuspended in 200 μl RPMI-1640 medium, 5% FCS, HEPES, pH 7.4, penicillin-streptomycin and glutamine, containing 50 ng/ml PMA (phorbol 12-myristate 13-acetate), 750 ng/ml ionomycin and 10 μg/ml brefeldin, and were incubated for 4 h at 37 °C 5% CO_2 in a 96-well plate. After stimulation, cells were washed with flow cytometry buffer and stained for surface molecules (CD4, CD8α and CD11a) overnight at 4 °C, then fixed and permeabilized in Cytofix/Cytoperm solution (BD Pharmingen). Cells were stained with antibodies to cytokines or their respective isotype-matched control antibodies. Samples were acquired on an LSR II (BD Biosciences). Data were analyzed with FlowJo Software (TreeStar).

Statistical analysis. The significance of differences between two groups was determined by two-tailed Student's *t*-test, or by one- or two-way ANOVA.

41. Luche, H., Weber, O., Nageswara-Rao, T., Blum, C. & Fehling, H.J. Faithful activation of an extra-bright red fluorescent protein in "knock-in" Cre-reporter mice ideally suited for lineage tracing studies. *Eur. J. Immunol.* **37**, 43–53 (2007).
42. Cui, Y. *et al.* Inactivation of Stat5 in mouse mammary epithelium during pregnancy reveals distinct functions in cell proliferation, survival, and differentiation. *Mol. Cell Biol.* **24**, 8037–8047 (2004).
43. Kaplan, D.H., Jenison, M.C., Saeland, S., Shlomchik, W.D. & Shlomchik, M.J. Epidermal Langerhans cell-deficient mice develop enhanced contact hypersensitivity. *Immunity* **23**, 611–620 (2005).
44. Murphy, K.M., Heimberger, A.B. & Loh, D.Y. Induction by antigen of intrathymic apoptosis of CD4$^+$CD8$^+$ TCR^{lo} thymocytes *in vivo*. *Science* **250**, 1720–1723 (1990).
45. Lutz, M.B. *et al.* An advanced culture method for generating large quantities of highly pure dendritic cells from mouse bone marrow. *J. Immunol. Methods* **223**, 77–92 (1999).
46. Omori, M. & Ziegler, S. Induction of IL-4 expression in CD4$^+$ T cells by thymic stromal lymphopoietin. *J. Immunol.* **178**, 1396–1404 (2007).
47. Bell, B.D. *et al.* FADD and caspase-8 control the outcome of autophagic signaling in proliferating T cells. *Proc. Natl. Acad. Sci. USA* **105**, 16677–16682 (2008).

© 2013 Nature America, Inc. All rights reserved.

doi:10.1038/ni.2541

Supp. Figure 1.

a

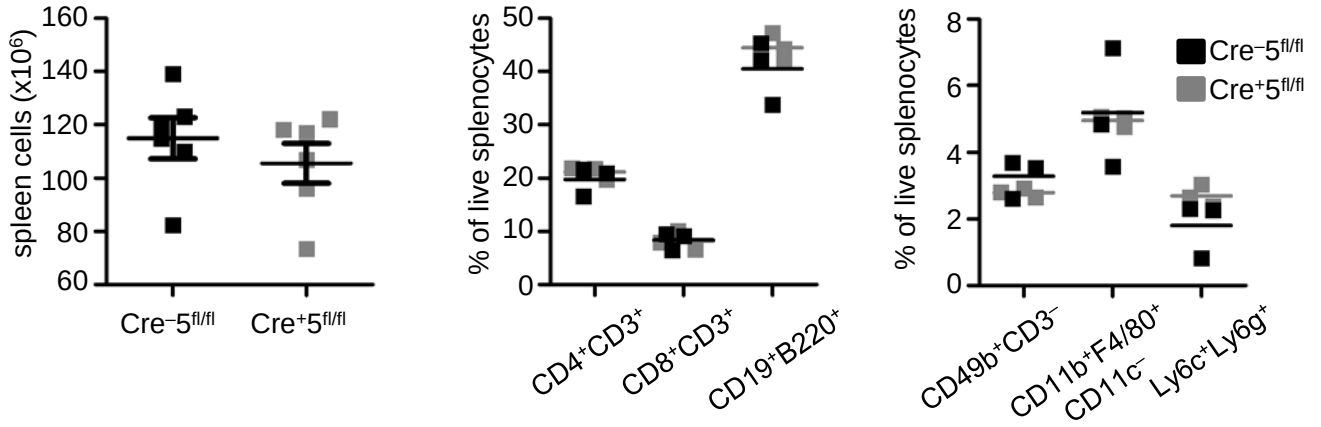

b

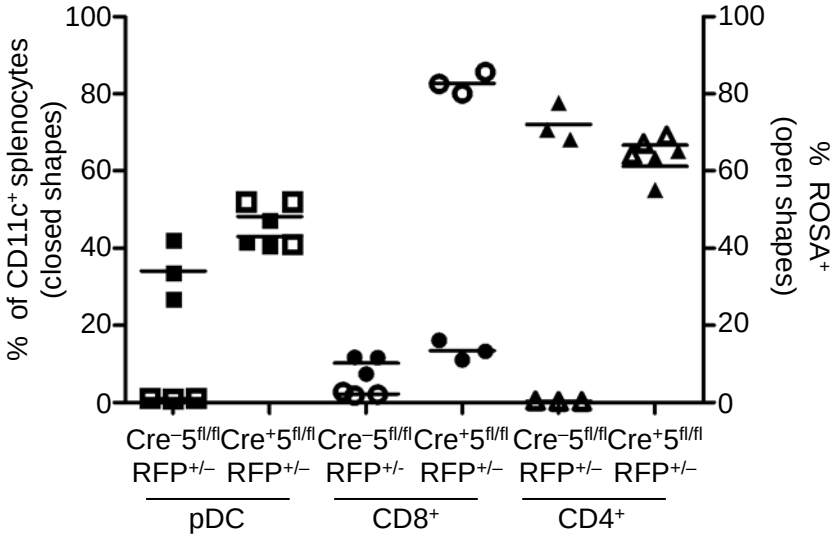

c

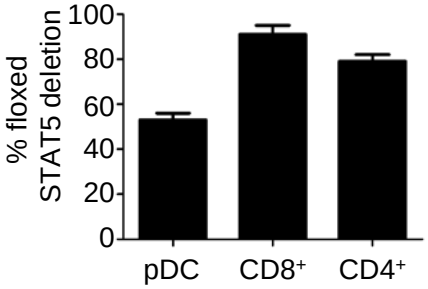

Supplemental Figure 1, STAT5 deficiency in splenic DCs has no effect on hematopoietic cell numbers. A, Total cellularity and percentages of hematopoietic cells in $Cre^{-}5^{fl/fl}$ and $Cre^{+}5^{fl/fl}$ mice. $CD49b^{+}CD3^{-}$ (NK cells), $CD11b^{+}F4/80^{+}$ (macrophages), $Ly6c^{+}Ly6g^{+}$ (granulocytes) Representative of three independent experiments. B, Percentages of pDC ($PCDA1^{+}CD11c^{+}$), $CD8^{+}$ DCs ($PDCA1^{-}CD11c^{+}CD11b^{-}CD8^{+}MHCII^{+}$), $CD4^{+}$ DCs ($PDCA1^{-}$ $CD11c^{+}CD11b^{+}CD4^{+}MHCII^{+}$) of total $CD11c^{+}$ splenocytes (closed shapes) and percentages of FLOX:STOP:RFP^{+} DCs within each gated DC population. Representative of three independent experiments. C, Deletion efficiency of STAT5 flox locus in sorted $Cre^{+}5^{fl/fl}$ splenic DCs. Graphed as percent of STAT5 flox allele deleted in the germline, in duplicate, representative of two experiments.

Supp. Figure 2.

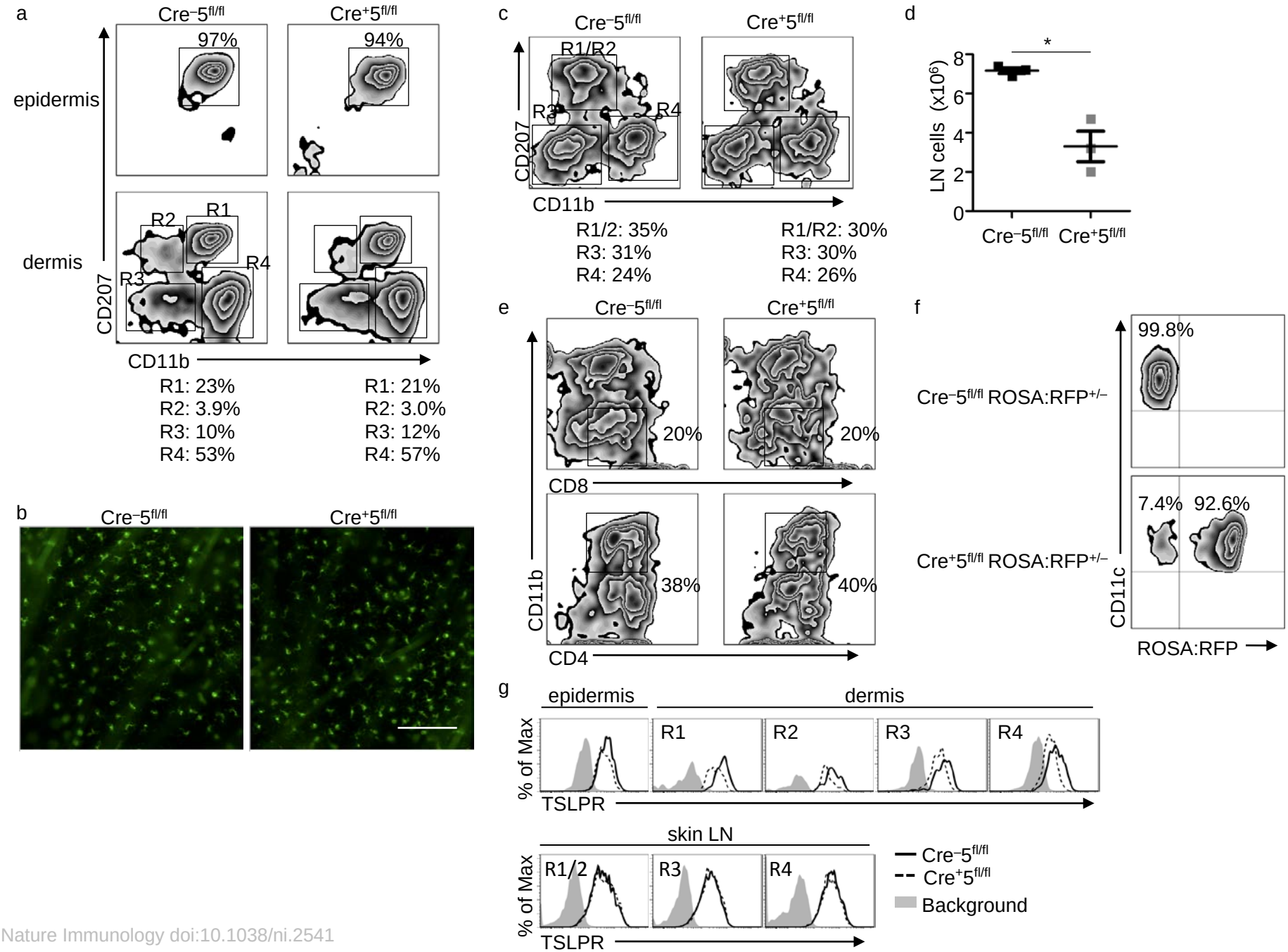

Nature Immunology doi:10.1038/ni.2541

Supplemental Figure 2, Normal skin DC development in $Cre^{-}5^{fl/fl}$ and $Cre^{+}5^{fl/fl}$ mice. A, $MHCII^{+}$ cells were analyzed for the expression of CD207 (langerin) and CD11b in the epidermis and dermis of $Cre^{-}5^{fl/fl}$ and $Cre^{+}5^{fl/fl}$ mice. Graphs and percentages are representative of three independent experiments. B, Fluorescent microscopy for MHCII in epidermal sheets. Scale bar is 100μm. C, Pooled axillary and inguinal skin dLNs from $Cre^{-}5^{fl/fl}$ and $Cre^{+}5^{fl/fl}$ mice were analyzed as in (A). D, Total cell numbers from pooled axillary and inguinal LNs from $Cre^{-}5^{fl/fl}$ and $Cre^{+}5^{fl/fl}$ mice. E, FACs plots gated on $CD11c^{+}$ cells. The percentages of $CD4^{+}$ and $CD8^{+}$ DCs from pooled skin dLNs of $Cre^{-}5^{fl/fl}$ and $Cre^{+}5^{fl/fl}$ mice, representative of three independent experiments. F, Percent of $CD11c^{+}$ DCs which are RFP^{+} from pooled axillary and inguinal LNs from $Cre^{-}5^{fl/fl}$ ROSA:$RFP^{+/-}$ and $Cre^{+}5^{fl/fl}$ ROSA:$RFP^{+/-}$ mice. G, TSLPR expression on epidermal, dermal, and skin-draining LN DCs of $Cre^{-}5^{fl/fl}$ and $Cre^{+}5^{fl/fl}$ mice are analyzed as in (A) and (C). Histograms are representative of three independent experiments. *p>0.01

Supp. Figure 3.

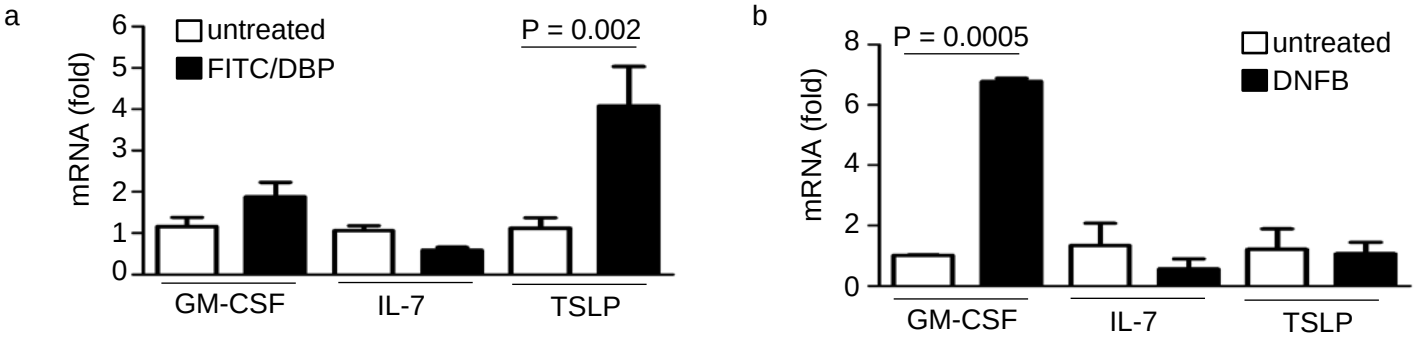

Supplemental Figure 3, Expression levels of STAT5 activating cytokines following CHS sensitization. A, WT mice were left untreated or sensitized on the ear with FITC/DBP for 24 hours, followed by qPCR for indicated STAT5 activating cytokines, normalized to HPRT and fold induction is relative to untreated ears. B, WT mice were left untreated or sensitized on the ear with DNFB for 24 hours, followed by qPCR for indicated STAT5 activating cytokines, normalized to HPRT and fold induction is relative to untreated ears. Minimum 3 mice per group, 3 independent experiments.

Supp. Figure 4.

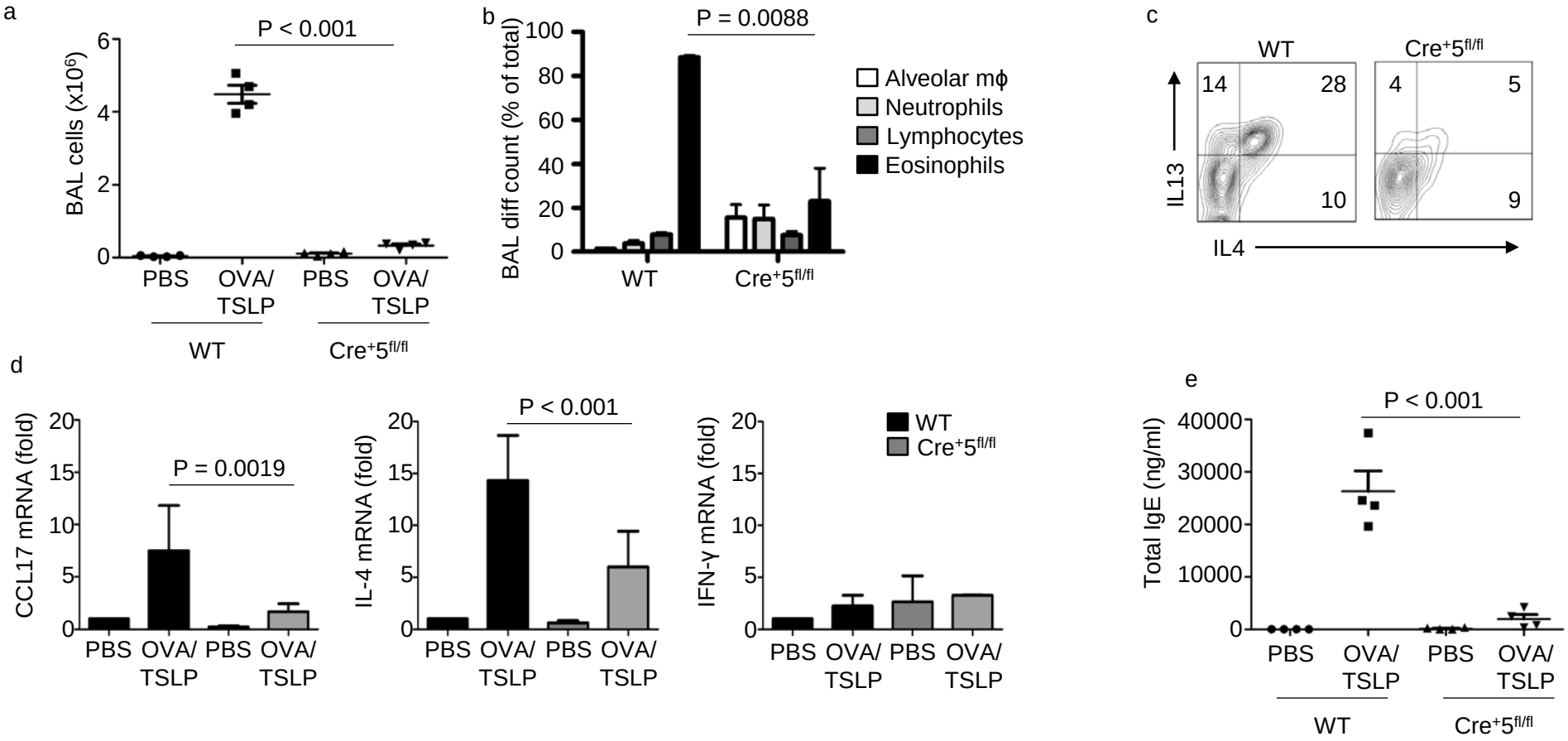

Supplemental Figure 4, Absence of STAT5 in DCs blocks TSLP-induced lung inflammation. A, Mice were treated with TSLP+OVA every other day for 7 treatments, followed by analysis 24 hrs after last treatment. BAL cell count (A) and diff count (B) were average of 4 mice per group. C, Intracellular staining of IL-4 and IL-13 following 4 hour restimulation. D, Expression levels of lung mRNA, relative to WT PBS controls. E, Serum total IgE in mice following last treatment. Two independent experiments with 3-5 mice per group.

Supp. Figure 5.

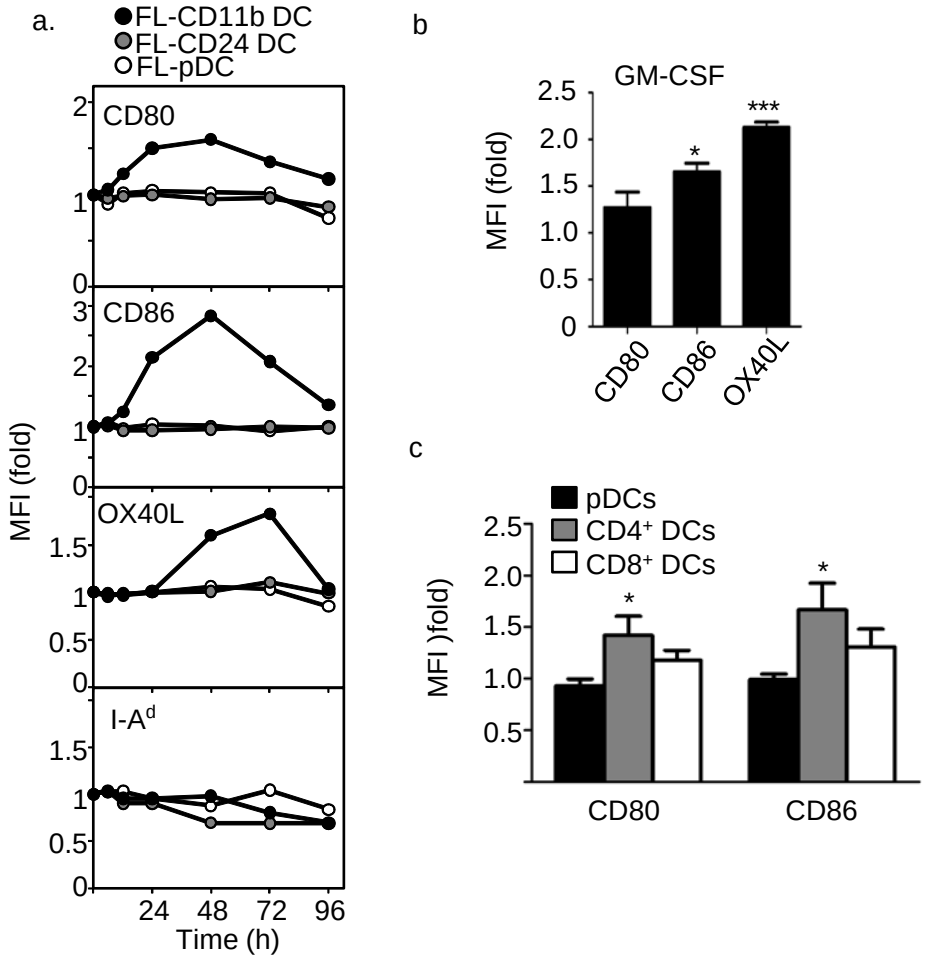

Supplemental Figure 5, TSLP activates specific DC subsets through upregulation of costimulatory molecules. A, Costimulatory molecule expression was determined by flow cytometry on FL-DC cultures over 96 hours following treatment with 50ng/ml TSLP or left untreated. B, Fold change in MFI of GM-CSF DCs following 48hr treatment with TSLP in triplicate. C, Fold change in MFI of the three splenic DC populations following TSLP treatment in triplicate. Representative of 3 independent experiments.

Supp. Figure 6.

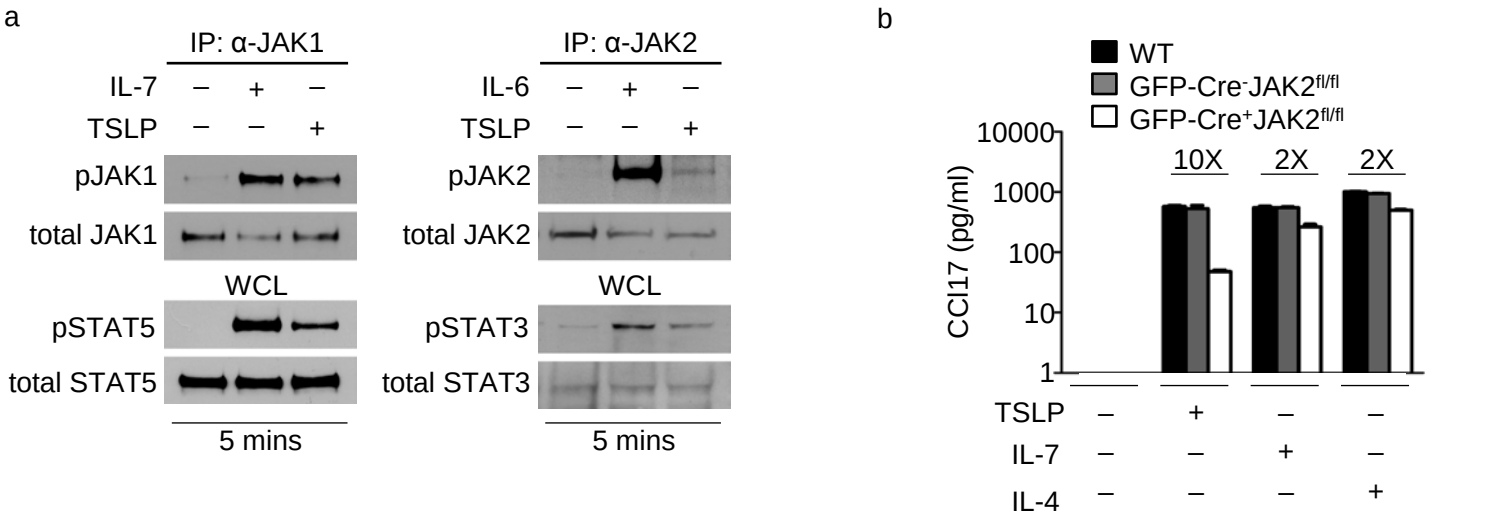

Supplemental Figure 6, TSLP activation of JAK proteins in FL-CD11b-DCs. A, CD11b-DCs were sorted from Flt3-L cultures and treated with 50ng/ml of indicated cytokines for 5 minutes. Whole cell lysates (WCL) were split into two, half were immunoprecipitated (IP) for indicated JAK, half were used as WCL control. Immunoblot analysis of indicated JAK and STAT phospho- and total-antibodies. Representative of 5 independent experiments. B, Jak2$^{fl/fl}$ FL-CD11b-DCs were infected with GFP-Cre retrovirus. 72 hours post TSLP treatment, CCL17 ELISA was performed on WT, GFP^{+} Jak2$^{fl/fl}$ and GFP^{-} Jak2$^{fl/fl}$ CD11b-DCs. Representative of two independent experiments.